Rain on Titan and its influence on splash erosion

The composition of rain drops and how they impact soil transport through splash erosion on Titan

Master Thesis

V.A.V.Jagarlapudi

Delft University of Technology

TU Delft

Rain on Titan and its influence on splash erosion

The composition of rain drops and how they impact soil transport through splash erosion on Titan

by

V.A.V.Jagarlapudi

Student Name	Student Number
V A V Jagarlapudi	5054710

Supervisors: Dr. Stéphanie Cazaux & Dr. Sebastiaan de Vet
Institution: Delft University of Technology
Place: Faculty of Aerospace Engineering, Delft
Project Duration: June, 2021 - July, 2022

Cover Image: Water splashing on wet sand + www.unsplash.com

TU Delft

Acknowledgements

There are so many acknowledgements I would like to make and hence, this section is comparably long to the rest of my thesis. That being said, here it goes.

My thanks begin firstly, to my parents and my family. My father, Kiran Kumar J P, for constantly inspiring me to follow my dreams and my interests regardless of what conventional instructions dictated back home. He was always supportive in my endeavours and never let the problems of home affect me in my most difficult periods during my thesis, standing by my side as he encouraged me to finish my research. My mother, Kiranmayi J, for having my back and reassuring me that I was never a burden, that I will finish my thesis and that I was never alone in this entire exercise. My little sister Vinuthna J, for always being around to listen to me and as a really good distraction with her own very teenager problems from back home.

I must thank my supervisors Dr. Stephanie Cazaux and Dr. Sebastiaan de Vet. You have always guided me, encouraged me and supported me during my thesis and helped me look at different aspects of a problem, some times going the distance to making me follow a decision that I did not fully understand yet, putting in the faith that I would do so eventually. Culturally, we are taught to respect our teachers and supervisors, in the form of a famous Sanskrit and Telugu verse, ఆచార్య దేవో భవ, which asks us to worship our teachers for the knowledge they give us. You have been an embodiment and served as a validation for this phrase. I can say that I feel immense gratitude to have worked under your supervision as I learnt to not only explore different depths of my work but also to enjoy it while I am at it. This gave me the inspiration to want to continue further in this same line of research. Thank you for inspiring me.

There is no home without its people and my dear roommate and friend Vishwanathan has lived up to this persona very well. It is therefore only asking that I thank you, my friend, for being there during all the times that were difficult, for checking up on me, for ensuring that I ate well and took care of myself as a good friend. You made me understand that there was more to sustain than academics alone and as many Indian students would understand, this is a very critical lesson that they would learn once they come abroad to study the way I did. Thank you for the many grocery shopping walks, many discussions we had over so many different topics and the many many meals we had together. Learning how to make dosa batter will be a big takeaway that kept me happy during some of the most difficult and uncertain periods of my thesis completion.

Next is my dear friend, Sai Saran Aduru. We were classmates from the very first day and as it happened, we struck a friendsip, one that I will cherish forever. Meeting you was one of the best things that happened to me at TU Delft because it made me realise that I was not alone in all the struggles we went together and that I had someone to talk about things. That you were always a phone call away for some very helpful advice was always an assurance and ensured that I did not make some of the mistakes many a predecessor of ours had made. I must also thank Poojitha for being a nice person to talk to and for always having a view (however controversial- the moon landing was not faked!) to argue about with me and for the many many meals we have had together, many moments we have all spent together, going out on small trips to the temple, or trips to a garden, many discussions, game/movie nights and the many pictures we have together (I still owe you guys a treat from my end). Thank you Saran, thank you Poojitha and thank the both of you together, for sticking around in very difficult times. You were friends when no one else was.

There is the thanks I must say to a few friends spread so far away, yet so close to my heart. One of them is Akshubhitha. You were always there, during the most mentally challenging phases and during the best times of my thesis, to encourage me or to simply listen to me rant, pushing me to make through the difficult times while you celebrated every small success of mine, regardless of their magnitude. I

have many thanks to owe to you and a trip that has been delayed for ever, to NYC. It will come soon. Another friend is Mythreya. My friend, my constant source of communication, of concerns from a world so different, I do not know how the years passed by with you. However, during my thesis, you would be there to listen to me and talk to me about different difficulties in life and constantly encourage me to speak out about things that bother me all the time. As someone who does not reach out very well, your advice was very encouraging, both to the person that is me and to my productivity. We too, will meet very soon. I look forward to it. A third friend I must thank is Anushruti Gupta. We met halfway through my thesis and you have already made such an impact in my life. I think you have witnessed closely my progress and listened to me constantly lose hope at every small setback, only pushing me to finish it and to do better at what I liked. Your constant belief in me made me believe in myself better and to raise my esteem bars to a level where I can confidently speak out my thoughts today, whether it was to my supervisors or otherwise. In a time so short, your influence has been magnanimous. For this, I can only say, thank you. I cannot end this paragraph without thanking my dear friend Umakanth. Mr. Popular, talking to you was always a fun thing and even though you never understood my thesis, you were the one I could always text for some advice on dealing with people, something that was a difficulty during my thesis. Talking to you was a constant source of reassurance. Thank you, for simply being you.

To Shiva Nischal, I must thank for always making use of your experiences to help me in my choices and to prevent myself from making mistakes. Your input and companionship during this master thesis is something I will always cherish.

My roommate Vinod, I thank you for being there during these times. Your perspectives opened my eyes to a different bunch of views and I always enjoyed our discussions during mealtimes.

To the people at BEST, thank you. You do not have an inkling of the influence you have had on me. You taught me to take life a little easy, to speak up for myself and to simply be myself. This really helped me implement my ideas better in the final stages of my thesis. I could not be looking more forward to working with you guys.

A few special mentions go out to Anshika, Subhadra and Harsh. Your friendship, advise and input is something I have always appreciated and cherished. Thank you for sticking around.

The world runs on people, (our) good and bad. We can only scale the heights of our successes with supportive people behind us. While that is a very double edged sword, this has been a very important lesson I have learnt during my thesis and I look forward to implementing in life. Thank you.

V.A.V.Jagarlapudi
Delft, August 2022

Contents

List of Figures

List of Tables

1

Introduction

When Christiaan Huygens discovered Titan, he knew not of the wonderful and intriguing world that the moon is. He also did not know that mankind would send missions in the future to study this little speck of yellow he saw in his telescope and in doing so, would honour his name forever by putting a lander on the surface of Titan. These missions were special because they were some of the very few missions sent out to explore the depths of our solar system. In that objective, they have sent back returns that have put forward our knowledge of planetary sciences by leaps and bounds. The Cassini-Huygens mission, directed specifically towards Saturn and its moons, returned a lot of information about its many moons and about Titan in particular.

Among the many things that make Titan intriguing is the presence of a dense atmosphere with a low gravitational acceleration. To put in context, the atmospheric density at the surface on Titan is 5.28 kg/m^3 [15] while that on Earth is 1.2 kg/m^3. The scale height for the atmosphere on Titan is 15 - 18 km [38] compared to 5-8 km on Earth [29]. The acceleration due to gravity on Titan is 1.354 m/s^2 [54] compared to 9.8066 m/s^2 on Earth. To add to this, traces of rainfall and precipitation have been found on Titan from the Voyager and Cassini missions.

Rain was first predicted to fall on Titan by Toon et al. [57]. At this time, it was posited that the rain drops primarily constituted methane [57, 55]. At that time, it was interpreted that rain drops formed out of very thin clouds and formed as aerosols descended through a supersaturated atmosphere [57, 37]. Later, once data from the Cassini-Huygens mission began flowing in, research indicated a change in the possible composition of the rain drop along with the possible mechanism of rainfall. The Huygens lander measured the distribution of methane in the atmosphere vertically [43, 42, 22] and it was shown that very humid and thick clouds of methane exist in the altitude range of 10 - 40 km [26]. Models began to indicate the possibility of rain drops accreting around an ethane nucleus, with the methane being sourced from methane clouds, meaning the methane cycle bore resemblance to the hydrological cycle on Earth in terms of drops forming from heavily saturated clouds [5, 4]. However, these models implied that rain drops on Titan could not be completely comprised of methane, owing to the presence of an ethane core. Furthermore, models [55] also began to suggest that rain drops consisted of a $CH_4 - N_2$ binary composition. However, the models could not predict an approximate distribution of the two components.

The combination of the density and gravitational acceleration as mentioned previously ensure that the rain drops fall at a slow speed on Titan, due to reduced acceleration and increased atmospheric resistance compared to Earth. This results in speeds of 0.5 - 1.5 m/s of rain drops that lie in the size range of 1 - 6.5 mm [26] by the time they reach the surface. This can be visualised in Fig. 1.1. This gives rise to a fascinating phenomenon of large rain drops falling in slow motion. This then raises the question of the impact of this kind of rainfall on other geological processes on Titan, since rain contributes in many ways to the geological processes on Titan. One such process is splash erosion.

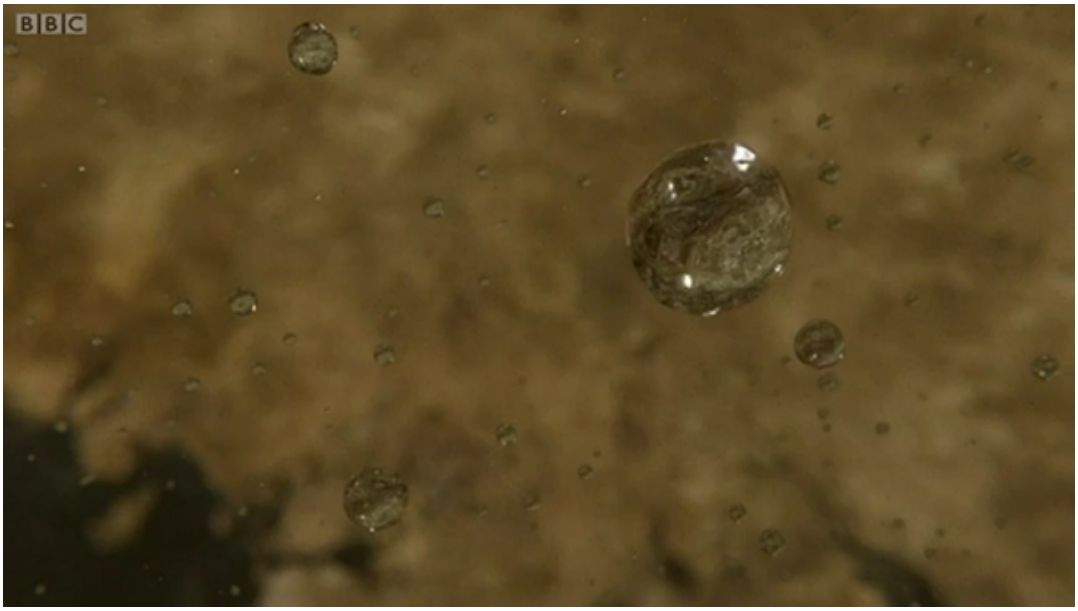

Figure 1.1: Artist illustration of Rain on Titan. Image credit: British Broadcasting Corporation (BBC) (BBC have done a beautiful short video introducing and visualising rain on Titan. It can be found here https://www.bbc.co.uk/programmes/p0070hxn).

Splash erosion is the erosion of soil layers by splashing liquid water. Commonly on Earth, this erosion is made possible by rainfall. Splash erosion as a phenomenon to be understood carries relevance since erosion is a process that contributes to continual displacement of soil on Earth. Combined with the hydrological cycles, it is possible to explain the kind of soil that is present in different locations on Earth depending on the geographic features of that location. The global phenomenon that contributes to the continual displacement of soil to various locations on Earth is commonly called sediment transport mechanism [48]. It is possible that such sediment transport mechanisms can exist on Titan as well. Attempting to understand this soil transport mechanism can help us map Titan's soil types across its surface, meaning that future missions to Titan can make use of this information. For example, landers such as the DragonFly mission [41] can make use of this information to determine suitable landing zones with better accuracy if the nature of soil and preceding geological activity can be predicted purely from visual inspection. However, determining the entire soil transport mechanism is a very large procedure and studying the impact of a single rain drop on the splash erosion taking place on Titan is a small contribution to that effort.

1.1. Research Question

In this thesis work, an attempt has been made to study the initial displacement of the soil particle through a falling solitary drop. In doing so, the work involves evaluating the possible amount of energy transferred to the soil along with the distance it has been displaced by the drop while splashing. This metric has been chosen for evaluating splash erosion on Titan since while the properties of rain drops and compositions have been evaluated, the rate of precipitation nor the frequency of precipitation has been firmly established. Therefore, under the assumption that the precipitation rate and rain frequency are similar to Earth, evaluating the energy possibly being carried away by soil due to rain allows us to understand how "effective" rainfall on Titan is. However, there needs to be a baseline parameter for this comparison to be coherent. This is why, the "performance" of rain on Titan will be compared to that of water. Combined with establishing a possible composition of the rain drop, understanding the contribution of rain to geological processes via splash erosion on Titan leads to the research objective. The research objective is summarised through the primary research question, which is

What are the qualitative and quantitative differences between rainfall on Earth and Titan and how does this difference reflect on the impact the drops have on soil?

This research question is driven by research sub-questions that better define the research objective and put it into perspective.

The research objective is to study the impact of rain on splash erosion on Titan by

1. *Estimating possible composition of rain on Titan*
2. *Evaluating if it is possible to obtain analogs of rain and soil to replicate Titan's rainfall in a laboratory*
3. *Measuring parameters that define splash erosion on Titan*
4. *Building models that predict the behaviour of soil on Titan after being subject to splash erosion.*

2

An Afternoon on Titan

Among the many moons that occupy orbits around various planets in the solar system, Titan occupies a unique position as being the only moon that has an atmosphere denser than the Earth at the surface [32, 15]. The density can be visualised in Fig. 2.1 through the fact that the surface of Titan cannot be seen through true colour images [17, 18]. This dense atmosphere is predominantly composed of methane along with a small percentage of nitrogen [15, 32]. In the upper regions of Titan's atmosphere, constant photolysis gives rise to various complex organic chemicals that exist in trace amounts within the atmosphere [52, 15]. These organic chemicals, form small particles of size range 0.7-10 μm that are the possible origins of rain drops on Titan [26, 55].

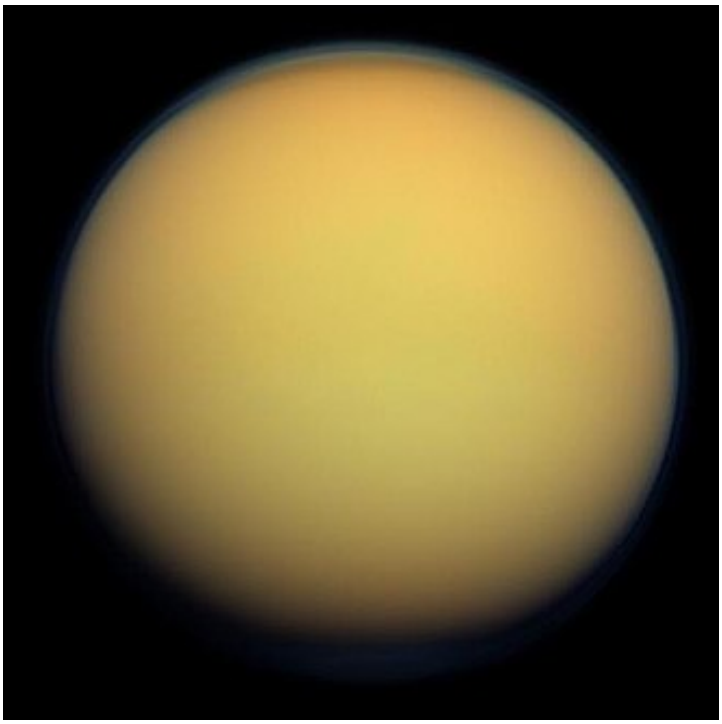

Figure 2.1: Titan, as captured by Cassini. Image credit: NASA/JPL

2.1. Titan's atmosphere

The Huygens lander, via the Gas Chromatograph Mass Spectrometer (GCMS) measured the mole fraction of methane in the lower atmosphere of Titan. The value at the surface was found to be 0.0565 $\pm$ 0.0018 or 5.65 $\pm$ 0.18% [42]. The variation with altitude is as shown in Fig. 2.2 below

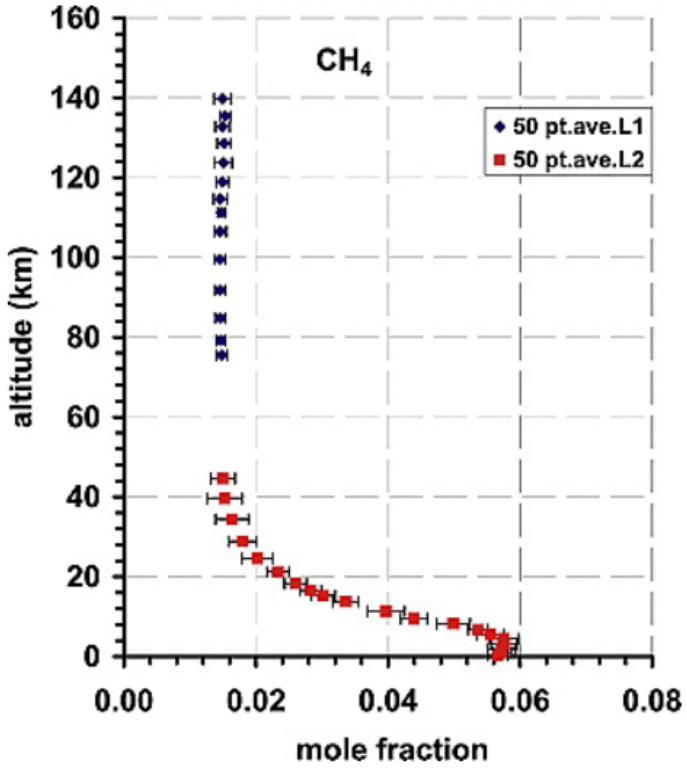

Figure 2.2: Variation of mole fraction of methane with altitude. The different colors of the measurements indicate the different sampling series or 'leaks' that took place during Huygens' descent. Image credit: Niemann *et al.* [42]

It can be noticed that the mole fraction of gaseous methane is lower at higher altitudes. This owes itself to the condensation of methane at these altitudes [29]. For better reference, the variation of temperature in the lower altitudes is as shown below in Fig. 2.3. It can be seen that the temperature rapidly drops in the stratosphere, eventually reversing the trend at an altitude of 40 km. The temperature here is low enough to facilitate condensation of methane. With atmospheric pressure increasing exponentially with decreasing height, methane should stay in the condensed form even though the temperature is increasing with decreasing altitude. Condensed methane sinks further in the atmosphere, increasing the mole fraction of methane in the lower atmosphere, contributing to an increase in the mole fraction with decreasing altitude. This means that the upper limit for cloud formation on Titan is at 40 km, as can be seen in Fig. 2.2. This conclusion is made since the mole fraction remains fairly constant above 40 km, meaning that it is possible that there is no condensation beyond 40 km.

2.2. Rain drop formation models

Condensate of methane particles should give rise to methane clouds on Titan. From measurements made by Coustenis *et al.* [16], ethane constitutes only 0.0015% of Titan's lower atmosphere. From a theoretical model built to predict the formation process of clouds on Titan by Barth *et al.* [6], it was understood that for methane clouds to form, they require nucleation sites for the aerosol growth to take place. The model then predicted that ethane coated tholins function as nucleation sites on which the cloud particle formation takes place, making ethane part of the 'core' of the cloud's aerosols. Further, the model points to a correlation between the composition of ethane in Titan's atmosphere and methane in clouds. It mentions that since ethane constitutes only about 0.0015% of Titan's atmosphere [16], the amount of methane present in the form of clouds is only 2% versus the methane that is present

in the vapor phase on Titan. Furthermore, the model also demonstrates that the methane that rises further up is destroyed via photolysis in the upper atmosphere (giving rise to other organic compounds as mentioned earlier) giving rise to the conclusion that the cloud formation cannot take place through the downward flux of methane from above. The cloud formation includes methane that rises from the surface or from the lower atmosphere alone.

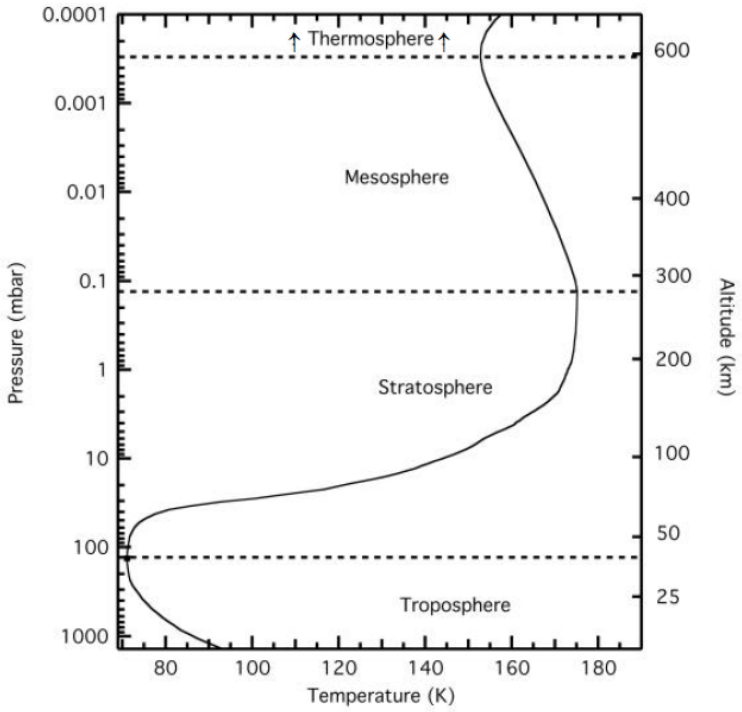

Figure 2.3: Variation of temperature of Titan in the lower atmosphere. Image credit: Horst *et al.* *,Horst2017TitansClimate*

The most relevant and modern model explaining the composition of rain on Titan is given by Graves *et al.* [26]. This is because it incorporates all existing models built to explain the mechanism of rain on Titan, addressing possible fallacies and merits to arrive at possible compositions of rain drops on Titan. It addressed the driving force behind the formation of a drop in the clouds. This is the mixing of methane and nitrogen at the cloud altitudes. This is made possible by the high relative humidity of methane (>80%) and nitrogen (>40%) at the mixing altitudes, which they posit to be in the range of 8-15 km. However, the conclusion of the outcomes from the models built by Graves *et al.* [26] is still uncertain because the relative humidity of ethane (C_2H_6) through out the atmosphere of Titan was not evaluated prior to the model being built, leaving Graves *et al.* to assume that the relative humidity of ethane is a constant value through out the vertical profile of the atmosphere. Thus, two cases were built for the simulation. One was the case of very low relative humidity of ethane in the atmosphere ($\rightarrow$ 0%) and the other was of high relative humidity ($\sim$ 50%). For a fall height of 8 km, Graves *et al.* [26] simulated the behaviour of a rain drop as it begins as a large drop and undergoes evaporation as it falls through the atmosphere and finally reaches the ground. The percentage of each compound in the drop is shown as the result of the simulation for two different cases, that are the relative humidity values of ethane through out the atmosphere. The results of these simulations are shown in table 2.1 below

Table 2.1: Properties of drops formed at different initial sizes for different relative humidities of ethane

	0% C_2H_6 (case a)	50% C_2H_6 (case b)
Drop radius at 8 km (mm)	4.75	0.92
Drop radius at ground (mm)	3.34	0.2
Fall time from 8 km (min)	78	361
Velocity at ground (m/s)	1.5	0.24
% Methane by mole at ground	77	40
% Nitrogen by mole at ground	23	20
% Ethane by mole at ground	1.8×10^{-8}	40
Drop temperature at ground (K)	90.0	93.5

In both cases, Graves *et al.* [26] lay down the possibility that rain drops can reach the ground. From the table, it is possible to estimate that a higher relative humidity of ethane through the atmosphere would result in greater evaporation of the drop as it falls through the atmosphere. The simulation results also nearly correspond with the claims made by Thompson [46] regarding the percentage of nitrogen within the drop as it approaches the surface. It was predicted to be around the $\sim$ 30% range and the simulation results for both cases of ethane relative humidity display that the mole fraction of liquid nitrogen within the drop is 20-23% of the drop. Establishing an approximate composition to estimate analogs for experimentation on Earth, will permit further study the influence rain drops can have on various geological processes on Titan.

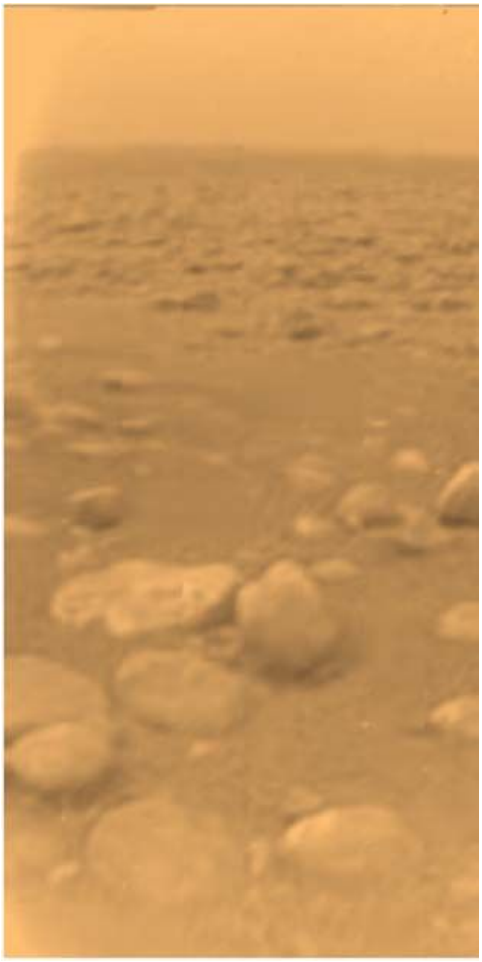

Figure 2.4: Image of Titan's surface as captured by the Huygens lander. Image credit: ESA

The soil on Titan is composed of a variety of organic compounds referred to as Tholins [30]. On a relatively flat surface that constitutes the moon [62], there is evidence of multiple soil transport mechanisms that could exist that determine the contextual nature of the outer surface of Titan, such as volcanic, tectonic and meteorite impact activities. Furthermore, models from optical, radar and infrared spectrometer images from Cassini [45] and the Huygens lander probe [56] have contributed in uncovering evidence of erosion brought about by flowing liquid on Titan [62]. Among the many mechanisms that constitute erosion, one is the contribution of rain in moving the soil on Titan, referred to as splash erosion. This forms part of the overall mechanism that moves soil on the moon, also referred to as the soil transport mechanism. Uncovering this possible contribution from the rain on Titan remains the goal of this thesis.

3

Methodology

The methodology entails the process of attempting to answer the research questions posed. In the introduction, it was mentioned that the contribution of a single drop to splash erosion, along with the division of energy between soil and splashing soil particles will be attempted to be studied. The plan through which this will be studied, or the thesis work flow, is visualised as shown below

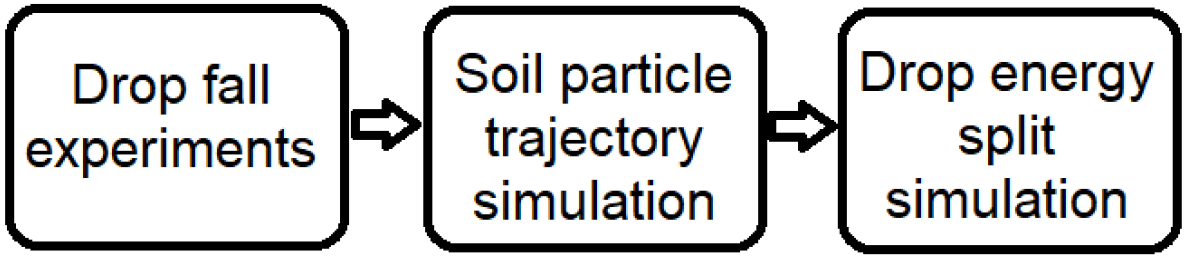

Figure 3.1: Thesis work flow

Each of these blocks depicted in Fig. 3.1 addresses one of the processes listed above. These processes and their respective attempts to address them during the course of this thesis are explained below

1. Drop Fall Experiments: The goal of these experiments is to basically simulate a falling rain drop as it would have been on Titan. These experiments pave the way to uncovering the initial part of the research objective in attempting to answer the research question, therefore providing certain observations that allow us to apprehend and quantify the consequences of apparent rain drops splashing on apparent soil of Titan. For this to be done, firstly, the rain drop composition is needed to be estimated. Hence, this work package is set up to answer certain questions and provide inputs for subsequent work packages. In setting up the experiments and performing them, it was aimed to achieve the following research objectives

    - Estimating possible composition of rain on Titan
    - Evaluating if it is possible to obtain analogs of rain and soil to replicate Titan's rainfall in a laboratory
    - Measuring parameters that define splash erosion on Titan

    In order to execute the experiments, certain steps were first taken to set them up. These are:

    (a) Establishing a possible composition of rain drops
    (b) Establishing a possible composition of soil on Titan
    (c) Evaluating possible analog compounds for experimental replication of Titan's rain drops and soil in Earth conditions

(d) Determining parameters to be measured and linking parameters to next phase of thesis work
(e) Determining experimental setup and experiment execution

Figure 3.2: Figure showing different stages of a drop splashing on a sample. Image credit: This work

Each of these steps are explained in detail in chapters 4, 5 and 6. The goal of this step is to visualise how the drop possibly interacts with soil. The measured parameters provide insight into how different they react with an approximate rain drop on Titan versus water. These parameters were then used to further the understanding of the soil displacement through the models that are built. During the course of this thesis, the chosen parameters were crater and splash diameter of the splashed soil (visualised in Fig. 3.3). The reasoning behind this selection will be provided in chapter 6. The choice of parameters influenced the subsequent models that were built to process the information obtained to quantify the drop's influence on soil displacement.

2. Soil particle trajectory simulation: Having collected the required parameters from the experiments, it now remains to process them. It was determined that in order to evaluate the energy carried away by the splashing mass of soil particles, it was necessary to first estimate the initial velocity of each particle. This is because a moving particle at the initiation of motion consists of kinetic energy which is the product of mass and the square of initial velocity of the particle. This means, that a fair assumption has been made, which is that a fraction of the energy of the falling drop has manifested into the kinetic energy of the particle, which is the only energy the particle possesses at the time of motion initiation.

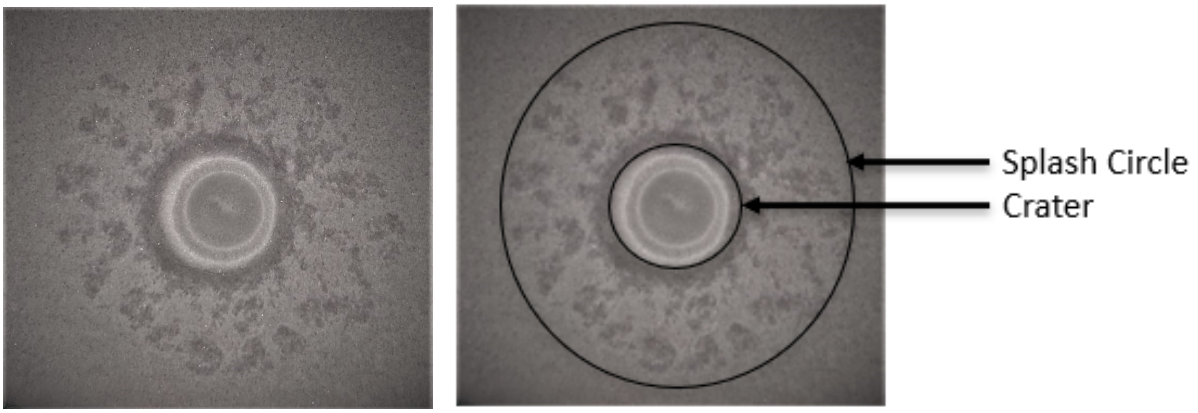

Figure 3.3: Figure showing soil splash samples and what crater and splash circle are. Image credit: Self

Therefore, the goal of this step is to determine the initial velocity of a soil particle at the time of

drop impact. This can be done since the diameter of the splash circle is known. However, not all particles fall at the periphery of the splash circle so multiple trajectories for various distances within the splash circle will be assumed, for which particle initial velocities will be calculated. Since analog conversion to mimic rain drops in the laboratory attempt to mimic the conditions on Titan, it is fair to assume that the drop-soil interaction is nearly accurate to how it would happen on Titan. This means that the initial velocity of the soil particle calculated for the experimental simulation would be nearly the same for a hypothetical particle on Titan. However, the splash distances registered in the laboratory would not be the same for a particle on Titan, due to the different atmospheric drag and gravitational acceleration at the surface. This means that by using the initial velocity and applying the model to fit for Titan's conditions, the trajectory of a splashing soil particle on Titan can be constructed. This would then shed light on possible splash distances of soil on Titan. This information is helpful because it helps us understand how far soil particles can get scattered on Titan and provides insight into how much the soil can be possibly displaced in a small rain shower.

However, in order to quantify the amount of energy the soil is carrying away, we need to estimate the amount of soil being displaced as well. This leads us to the next block shown in Fig. 3.1.

3. Drop energy split simulation: Having obtained the initial velocity of the soil particle, estimating the mass of the splashed soil will complete the study, who's goal is to estimate the energy being carried away by the soil per splashing drop. Since the energy carried away by a single particle is approximately known and the drop-soil interaction in the lab is akin to that of that on Titan, the total mass of the carried away soil in experimental conditions can be assumed to be similar to that on Titan. Now, in order to estimate the mass of the soil being displaced, properties of the soil need to be established. In this case, it is the detachability factor of the soil. The relevance to this is explained in chapter 7. Once relevant parameters are established, the mass of the soil scattered in the entire splash circle can be calculated.

   From the mass of the soil splashed, the total energy carried away by the splashing soil can be calculated since the energy carried away per particle depending on splash distance is known and hence, the total energy carried away by the particle can be estimated. Once this is done, the ratio of energy of splashed mass to energy of the drop can be calculated. This allows the energy values to be contrasted to the initial energy of the drop, allowing us to evaluate how much of the drop's energy is the splashing soil carrying away. For quantitative purposes, this is referred to as the "performance" of the rain analog.

These two work packages aim to answer the final research objective goal, that is

- Building models that predict the behaviour of soil on Titan after being subject to splash erosion.

Having established the flow of work for reaching the end goal of the research question, this methodology details to explore how the environment on Titan surrounding the drop-soil interaction can be best replicated in order to simulate the behaviour of Titan's soil to falling rain drops.

4

Composition of a rain drop on Titan

Graves *et al.* [26] created a model that shows that a droplet of rain on Titan contains a mixture of $N_2 - CH_4 - C_2H_6$ (Nitrogen, methane and ethane). With this mixture, assuming different values of fixed relative humidity (0% and 50% by mass) of ethane in the atmosphere, it was concluded that the rain drops underwent growth in the altitude region of 8-15 km. Above this region, the rain drops are formed on cores of sizes not larger than 10 μm [5]. Furthermore, methane clouds form at altitudes below 40 km [42]. At altitudes below 40 km, the relative humidity of ethane appears to vary between 0% and 5% [53, 59]. At this altitude range, the mole fraction of ethane appears to vary in the following manner as shown in Fig. 4.1. It can be seen that the mole fraction drops significantly from altitudes lesser than 100 km, experiencing a reversal at 50 km, and drops once again below 30 km. It can also be seen that between 30-70 km, the mole fraction of methane is high enough for methane to be saturated. Also, the temperature profile drawn for the droplet assumes a composition of 40% methane-20% nitrogen-40% as mentioned before, which is not the composition for the case of low relative humidity of ethane. This temperature profile therefore, is lacking in terms of the appropriate relative humidity of ethane.

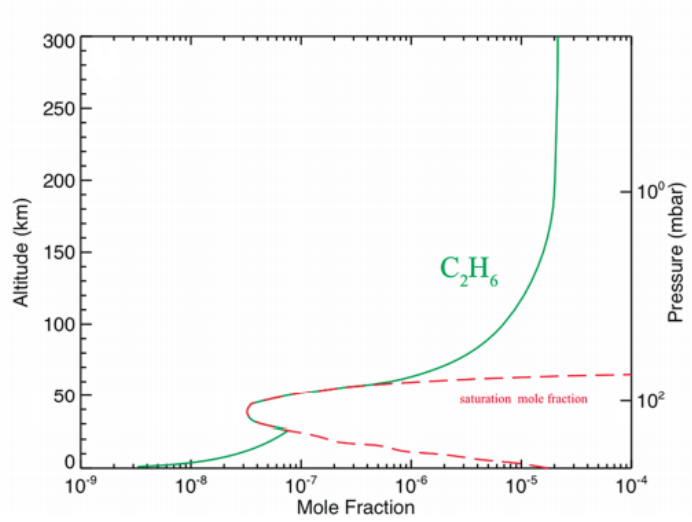

Figure 4.1: Variation of mole fraction of ethane along with the saturation mole fraction, subject to variation of pressure and altitude as modelled from Cassini's observations. Image credit: Wilson *et al.* [59]

However, methane cloud formation and precipitation takes place at altitudes below 15 km [26]. The growth of a cloud particle i.e accretion of condensing methane and nitrogen on an ethane core takes place at altitudes below 15 km until 8 km. This could imply that ethane descends from the altitude of saturation ($\sim$ 60 km [53]) towards the surface and accretes methane and nitrogen along the way, forming the rain drop. However, the low relative humidity (< 50%) of ethane in this region limits the stability of the rain drop formed by the mixture. The difference in partial pressure of ethane within the

raindrop and the surrounding atmosphere is used to determine the evaporation rate as shown in Eq. 4.1.

Graves *et al.* [26] assumed that the ethane nuclei mixes completely with the rest of the liquid droplet, forming a homogeneous mixture and that this mixing process does not influence the balance of thermal energy within the drop. For this, the evaporation rate for a falling drop is computed using the following relation

$$\frac{dM_i}{dt} = \frac{f_v 4\pi a_0 D_i m_{di}}{RT_f}(P_{vapor} - P_{di}) \tag{4.1}$$

Where i is the compound for which we are evaluating the evaporation rates and P_{vapor} and P_{di} are the atmospheric partial pressure and vapor pressure of i in the drop. The relative values of P_{vapor} and P_{di} control the sign of dM_i/dt, and therefore whether the drop is gaining or losing the component i. The other terms in Eq. 4.1 are the ventilation coefficient (f_v), drop radius (a_o), diffusivity coefficient of i (D_i), molecular mass of i (m_{di}), universal gas constant (R), and T_f=(T_{atm}+T_d)/2, where T_{atm} is the air temperature and T_d is the drop temperature.

Here, ventilation coefficient is the product of maximum mixing depth and the wind speed at a particular altitude. Maximum mixing depth is a mathematical value obtained by projecting the dry adiabatic lapse rate on the planet and the temperature profile of the planet. The point where the two lines first intersect corresponds with a certain altitude (as the lapse rate and temperature profile are extracted with respect to altitude) and this altitude is referred to as Maximum mixing depth or mixing height [2]. The ventilation coefficient is attributed a value of 15 in the growth region and 1 in the region where it undergoes free fall after the growth region in the calculations done by Graves *et al.* [26].

At this point, Graves *et al.* [26] ran two trials (for the two values of relative humidity of ethane in the atmosphere) of rain droplets falling from an altitude of 16 km for particles of different seed (ethane) sizes. The seeds grew in the growth region according to this hypothesis until an altitude range of 10-8 km after which, they began to subsequently evaporate during their descent till the ground. Of the drop sizes that made it to the ground, it was noted from the trials that in the case of a constant relative humidity of 0% of ethane, a drop of diameter 3 mm and lower at an altitude of 8 km failed to reach the ground while in the case of a constant relative humidity of 50% of ethane, the drop reached the ground, having shrunk significantly. This implies a significant dependency of the survival and size of the droplet on the vertical relative humidity profile of ethane.

Graves *et al.* [26] claim that large drops (> 3 mm radius at formation height) impact the surface at 1.5 m/s but do not shed light on the minimum size that a drop required to cause substantial soil erosion (displacement of unit quantities of soil). Furthermore, it has been mentioned that lower relative humidity of ethane implies greater drop size as smaller sizes of droplets evaporate. Linking the fact that there is rain on Titan with the presence of splash erosion evidenced by the formation of drainage and flow patterns on Titan will serve as a confirmation for the calculation done to establish the size of the rain droplets on Titan. Further, it will also serve as a basis to make a conclusion concerning rainfall patterns at various locations across the surface of Titan. This aspect linking size of rainfall droplets (factoring in the profile of the relative humidity of ethane) to the formation of splash erosion patterns is absent in literature, serving as a potential gap in which further research can be done.

4.1. Reasoning and possible composition

Previous simulations as shown by Graves *et al.* [26] laid out two cases detailing the possible outcomes with which rain droplets arrive at the ground. In their scenarios, they had assumed a constant relative humidity of ethane in the atmosphere, at 0% and 50%. The actual variation of the relative humidity of ethane in the atmosphere of Titan has been evaluated by Tokano [53] using the Cologne Titan General Circulation Model (GCM). This model obtained the mole fraction of ethane, from which the relative humidity was computed by Tokano [53] using the observations made by the Cassini Composite Infrared Spectrometer (CIRS) via the following model used to determine the mole fraction of ethane in

the uppermost layer of the atmosphere (C_{top}).

$$C_{top} = max(1.5 \times 10^{-5}, 1.5 \times 10^{-5}[1 + 2cosL_s sin\phi^3])$$

Here, L_s is the solar longitude of Titan and ϕ is the latitude. This mole fraction is passively introduced into the GCM model is subject to three dimensional advection and loss due to condensation. Thus, the mole fraction and subsequently, the relative humidity of ethane in the atmosphere across altitudes is computed.

The rain drop composition is influenced by the pressure and temperature profiles on Titan. It is also influenced by the density of the components. The difference between the temperature of the rain droplet and the atmosphere dictates the heat transfer rate between the droplet and the atmosphere and this in turn, shows us whether the rain drop is evaporating or not. Interestingly on Titan, the conditions favour the growth of the rain droplet in the altitude region of 16-8 km. This is made possible by a combination of the various conditions in this region; the temperature increases from 78.88 to 84.72 K and the pressure increases from 0.612 bar to 0.961 bar as the altitude reduces (Model for Titan's atmosphere consisting of 3% CH_4, 2% Ar, 95% N_2 by Yelle *et al.* [60]). The models determined by Yelle *et al.* [60] are computed using the Radio Science Subsystem (RSS), Infrared Spectrometer (IRIS) and the Ultraviolet Spectrometer (UVS) packages onboard the Voyager I mission. This trend of increasing temperature and pressure continues all the way till the surface. This can be seen in Fig. 4.2

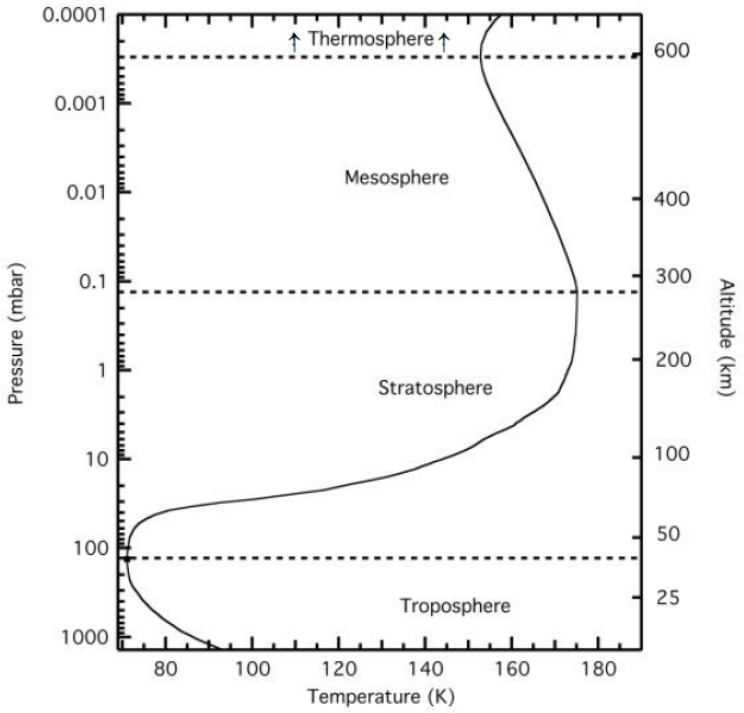

Figure 4.2: Variation of temperature and pressure on Titan. Image credit: [29]

Therefore, it has to imply that the temperature and pressure can set the boundary regions defined by altitude (since they vary as a nearly linear function of altitude in the lower troposphere as can be seen in Fig. 4.2). However, the growth in this region is made possible by the high partial pressure of nitrogen and methane, which can be inferred from their high relative humidity in this region. The variation of the mole fraction of methane and nitrogen on Titan with the altitude has been computed by Graves *et al.* [26]

On observing the high relative humidity in the growth region, it can be concluded that the relative humidity is a deciding factor on the size and existence of the constituents of the droplets in their respec-

tive phases.

From the cases outlined, by Graves *et al.* [26], we now have two possible compositions for the rain droplets for two assumed scenarios of relative humidity of ethane. The two compositions can be seen in Table. 2.1.

The two cases arose owing to the uncertainty in the actual variation of the relative humidity of ethane. Both cases assume a certain constant value of relative humidity of ethane through out the entire altitude range of Titan. The variation in relative humidity has been published by Tokano [53] in May, 2021. From Tokano's estimation [53], the variation of the relative humidity in the atmosphere of Titan has been determined across all latitudes. The variation however, cannot be seen accurately in the lower troposphere. This variation has been magnified and shown for every latitude in Fig. 4.3

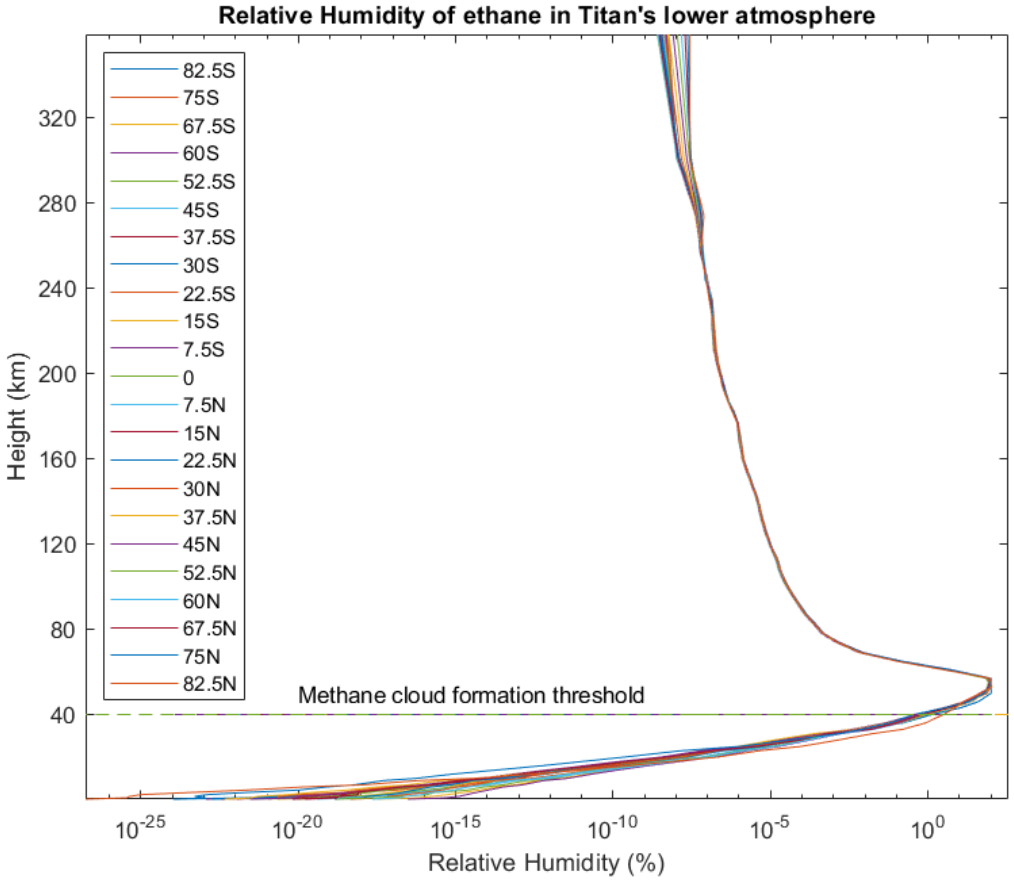

Figure 4.3: Estimated variation of relative humidity of ethane at all latitudes. The data in this figure has been provided by Mr. Tetsuya Tokano, Staff at the Institute for Geophysics and Meteorology, University of Cologne. This data has been implemented in literature [53]

The bump that can be seen at an altitude of $\sim$ 60 km is caused by rapid condensation of ethane while descending into the atmosphere. This descent is caused by a global atmospheric circulation driven by thermal imbalances between tropical and polar areas, setting up a circulation mechanism similar to Hadley's cell [53]. During the descending leg of this cell, air descends into the troposphere and at an altitude of 50 - 60 km, or about 10 km above the tropopause, the temperature lapse rate is high enough to cause rapid condensation of ethane, as a result of which, the relative humidity in this region appears to be supersaturated [29]. This lapse rate can be visualised in Fig. 4.2. This supersaturated phase is a very widespread phenomenon (globally) during late summer and winter [53]. Considering each season lasts an approximate 29 years [32], this vertical profile of ethane's relative humidity

on Titan is assumed to be a constant setting for studying short term rain and its consequences on Titan.

From Fig. 4.3, it can be seen that the relative humidity of ethane in the lower troposphere of Titan is varying in the magnitudes of 10^{0} to 10^{-26}. These values are so low that they can be approximated to 0% for the sake of inferring the composition. The relative humidity is considerably constant over the entire altitude region that comprises of the droplet formation, growth and fall, implying that this is comparable to the inferences drawn by Graves *et al.* [26]. Since every other influencing parameter is drawn with reference to the work done by Graves *et al.* [26], it can be concluded that the composition of the rain droplet follows that of the composition laid out in table 2.1 for the case of 0% relative humidity of ethane. Thus, the composition is, by mole fraction, 77% of methane and 23% of nitrogen.

5

Rain and soil in a Titan on Earth

5.1. Analog for rain drops

Having arrived at an estimate for the composition of the rain droplet, it has now been defined what approximately is the density and the other properties of rain droplets on Titan. This has been brought by putting relevant literature together and using the available data to come to the conclusion as explained in the previous chapter. Now, to recreate this liquid on Earth for the sake of experimental studies, we need to create an analog of this liquid. The necessity for the analog is due to the following factors

1. Change in acceleration due to gravity from Titan (1.354 m/s^2 [54] to Earth (9.8066 m/s^2)
2. Changing atmospheric temperature of Titan at the surface (90 K [26]) and Earth (298 K)
3. Changing surface pressure of Titan (1.5 bar [26]) and Earth (1.013 bar)
4. Changing atmospheric density of Titan (5.28 kg/m^3 [15]) and Earth (1.2 kg/m^3)

In order to mimic the rain of Titan on Earth, it is necessary to translate the various properties of rain droplets from Titan to Earth. Scaling however, must be done by maintaining certain properties identical. Therefore, all other properties are scaled appropriately. The properties are listed below

- Surface tension: The cohesive forces present in the rain droplet need to be the same in the rain droplet falling on Earth. The same force allows us to perceive the impact the rain droplets have on the soil.
- Drop radius: The drop radius is necessary to be conserved across, as the size of the impact being generated on the soil influences the amount of soil being spread and subsequently, displaced.

These properties are reflected for the final computation of droplet properties that reach the ground on Titan. The droplets have undergone evaporation as they fall to the ground and finally arrive with properties outlined by Graves *et al.* [26] and these values are computed in Table. 2.1. The properties that are maintained from Titan to Earth (mentioned above) are reasoned to carry across the influence of the rain droplet on the soil from Titan to Earth. Therefore, all other parameters are scaled. In order to ensure that the energy of the droplets is conserved, droplets are scaled with respect to height of release in the experimental setup. This means that different droplets will be left from different heights in order to ensure that the droplets strike the soil at the same energy as they are expected to do so on Titan.

Now drop radius is a geometric property and hence can be replicated regardless of the analog liquid being implemented. Surface tension on the other hand, is an intrinsic property of the compound and hence, specific liquids will be used in order to mimic the surface tension of the Titanian rain droplets. From Baidokov *et al.* [3], the surface tension of the rain droplet has been estimated to be 15 mN/m. Now, the atmospheric conditions were scaled such that the conditions mimicked room temperature on Earth. These are

- Temperature of atmosphere at ground: 298 K

- Pressure of atmosphere at ground: 1.1013 bar
- Atmospheric density at ground: 1.2 kg/m^3

At these conditions, analogs for the rain droplet liquid were searched for. On searching and evaluating potential candidates to serve as an analog, two compounds were singled out. They are

1. Ethanol (C_2H_6O)- 21 mN/m ([27])
2. n-pentane (C_5H_{12}): 16 mN/m ([27])

In order to contrast the results with rain on Earth, water will be used to study the influence it has on the Titan soil analog. This allows to set a reference measure for the results we calculate for various analogs.

5.2. Analog for soil

In order to arrive at a suitable analog compound for the soil on Titan, it is necessary to first estimate the possible composition and physical properties of the soil on Titan. From data gathered through the impact penetrometer of the Surface Science Package on the Huygens lander that touched the surface of Titan in 2005, it was gathered that the surface of Titan is typically flat around the landing zone, but not uniformly so [62]. It is expected to be mostly composed of organic sediments, commonly tholins [62, 33, 61]. Further study has placed the soil particle density within a range of 500 - 1400 kg/m^3 [61, 30, 31, 28].

For this particle density range, obtaining an analog on Earth implies that a suitable compound should have the same weight on Earth so the particles being splashed carry approximately similar amounts of kinetic energy as a soil particle would on Titan for a drop of similar energy. Weight is a product of mass and gravitational acceleration. This means that for particles of similar diameter as the soil particles on Titan, the particle analogs on Earth need to compensate the increase in gravitational acceleration from Titan to Earth by reducing the particle density. The density will be reduced by a factor of approximately 7.5, which is the ratio of the gravitational acceleration on Earth to Titan (if acceleration on Earth is higher, then particle density on Earth is lower, since weight is the product of mass and gravity and mass is directly proportional to density of particle). Therefore, density of the soil particle becomes the scaling property across which every parameter is scaled.

Through experimentally gathered inferences, Burr *et al.* [9] estimated that the soil particles on Titan should possess a size range of 60 - 600 μm. This was gathered based on Cassini's observations of dune sand on Titan, meaning this size range is restricted to sand particles that have been subject to constant wind transportation. There is no complete understanding of soil particle size on Titan, since the size of the ice particles that constitute the surface of Titan have not been estimated on a global scale [35], [9].

Yu *et al.* [61] compared different possible analogs and mention the implementation of hollow glass bubbles lying in the particle density range of 100 - 140 kg/m^3. The glass bubbles listed in the literature are expected to have a size range of 30 - 115 μm. The usage of glass bubbles is also corroborated with their usage at the Titan Wind Tunnel [10] [9] for recreating the soil of Titan for aeolian studies.

While selecting a particular value of density and size of particles for the glass bubbles to be used in the experiments, there was limited choice. In the expected size range and density range, there was a single combination of glass bubbles that were available for purchase. **Thus, the glass bubbles obtained for experimentation purposes consist of a median diameter of 65 μm and a median density of 120 kg/m^3.**

6

Setting up experiments with boundaries

Having established possible analogs to replicate the rain and soil on Titan in Earth based conditions, it is now necessary to develop experiments that can put these analogs to use such that observations on the interaction of rain with soil on Titan can be observed in lab conditions. Hence, it is first necessary to define the nature of the experiments.

6.1. Experiment definition

1. The experiments aim to study the influence of a falling droplet onto the soil sample and in doing so, measure the amount of soil displaced horizontally in the form of the crater and splashing material (visualised in Fig. 3.3 via analog instruments - vernier calipers).
2. The experiments aim to establish the relationship between drop energy and soil splash displacement and energy.
3. The experiment intends to mimic the behaviour of drops of size ranging between 2 mm and 3 mm, or drop radii falling in the range of 1 mm to 1.5 mm functioning as a rain drop analogous to ones on Titan. These drops will be reaching the ground with predefined velocities based on drop velocities at ground for drops on Titan. These values result from numerical simulations in literature [26, 37] and evaluate their behaviour based on their displacement of a soil sample that is an approximate analog of the soil on Titan.
4. The soil is placed on a platform that is level with the ground.

6.2. Experimental boundaries

The boundaries and the assumptions that are considered, going forward with the experimental process are as follows

1. A single drop falls on a soil sample in each experimental iteration
2. The drop is unaffected by forces such as drag and does not split into smaller droplets because of resistance forces - a single drop always arrives at the soil sample in each iteration.
3. The drop does not undergo a change in temperature, surface tension, internal pressure or phase.
4. The soil is at a fixed temperature, pressure and density and is placed on a bed that is at 0° inclination.
5. There is no lateral force acting on the drop- wind is not considered to exist in this experimental simulation.
6. The entire drop falls on the soil sample alone.

A pipette that holds drop at different heights will be mounted on a chemical stand such that the height of the pipette can always be adjusted. The setup is placed in a fume hood. The volume of droplets falling varies from 4.18×10^{-3} μm^3 to 14.13×10^{-3} μm^3, or 4.18 μL to 14.13 μL for every analog. A single pipette will be used to let go of a single drop from the desirable height to approach the soil sample. The stand will be accompanied by a scale to measure the height of the pipette to accurate dimensions in

order to ensure the drop with the right amount of kinetic energy reaches the floor for a particular drop radius. This setup is seen in Fig. 6.1

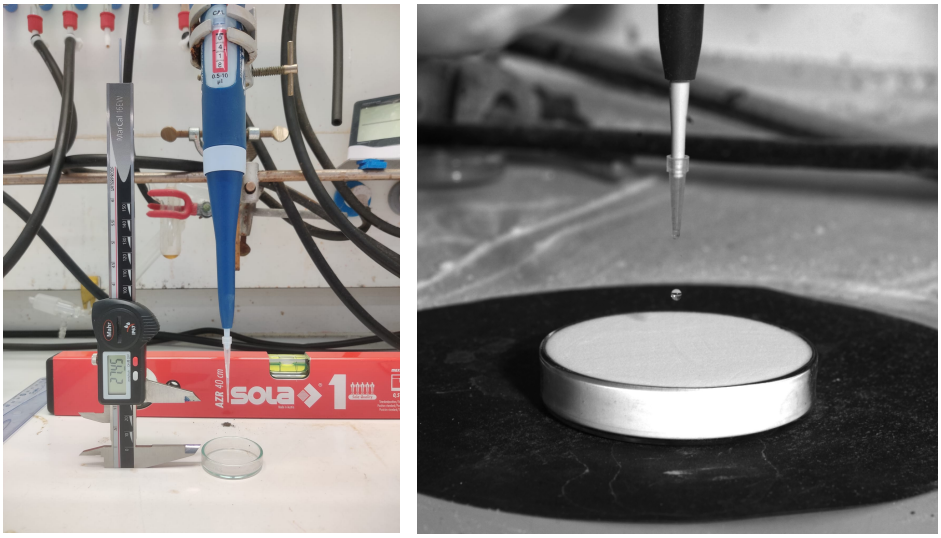

(a) Setup with physical boundaries defined **(b)** Setup being implemented with soil analog

Figure 6.1: Experimental setup

6.3. Setup elements

6.3.1. Pipette

The instrument to generate the rain analog drops was chosen to be a mechanical pipette. For the required drop volumes, a VWR single channel UHP pipette (part number: 613-1490) was chosen. The volume range of this pipette is $10 - 100$ μL.

Figure 6.2: VWR single channel UHP pipette. Image credit: VWR https://nl.vwr.com/store/product/7551375/eenkanaalspipetten-mechanisch-variabel-volume-ultrahoge-prestaties-uhp#gallery-6

6.3.2. Pipette tips

The pipette is capable of holding the desirable volume of rain analog. But this does not assure that the volume of liquid is released in a single drop. This is made possible by manipulating pipette tips. The reasoning behind this is the fact that increased circular diameter of the pipette tip contributes to increased size in drop generation [58]. Since the tips are conical in shape, by cutting off a portion from the bottom of the tip, it was possible to obtain a wider tip of the pipette, meaning a larger drop could be generated. This meant that in order to obtain a larger drop, the tip had to be cut shorter. This can be seen in Fig. 6.3. Through trial and error, various tips for different drop sizes for different analogs were made. Since different analogs and water have different values for surface tension, this meant that each analog had to have its own tips. For 3 sizes of drops and 3 different liquids, this meant that 9 different tips were required.

Figure 6.3: Pipette tips for ethanol, for drop of radii 1.25 and 1.5 mm. It can be seen here that the tip used to produce a drop of 1.5 mm radius is shorter and has a broader opening at the end.

6.3.3. Soil sample preparation

The technical documentation [1] (in German) mentions that the volumetric packing density of the glass bubbles is in the range of 55% - 68%. On free packing of the bubble sample into a petri dish, it was noticed that the samples had a mean packing density of 62% (assuming the bubbles were uniformly distributed through the dish). On using this sample, it was noticed that the experiment results were not consistent. There were regions where it was slightly more densely packed and regions where it was not packed sufficiently meaning the observations after the experiments were conducted were not uniform for multiple drops of the same size and fall height (drops of the same size and fall height can be expected to splash similar amounts of soil analog sample), as can be seen in Fig. 6.4a. It was then concluded that the bubbles were not packed uniformly.

In order to obtain uniform distribution of the bubbles, they had to be packed uniformly into the dish. Doing so raised the amount of sample required to fill the dish to the brim. This meant that there would be an increase in the uniform packing density as well. In order to determine the packing density at which the results were uniformly obtained across the dish, the amount of sample that was packed into the dish was increased by trial and error by manipulating the mass through the packing density. This was made possible easily because the glass bubbles are very small and simply by tapping at the sides of the petri dish, it was possible to pack greater amounts of sample into the dish which increases packing densities. However, over packing also becomes a problem then because the sample becomes too tightly packed to observe any significant soil splashing. Thus, the sample packing density had to be minimal to allow for sample splashing but large enough to ensure uniform distribution and experiment reproducability. At a packing density of 64% $\pm$ 0.5%, it was first observed that the results of the drop experiment across the sample (and across various analogs and water) yielded homogeneous results as seen in Fig. 6.4b. Therefore, this became the benchmark value used consistently for all drop sizes across analogs. For a petri dish of diameter 178 mm and depth 11 mm, this meant that the mass of the sample lied in a range of 4100 $\pm$ 50 g.

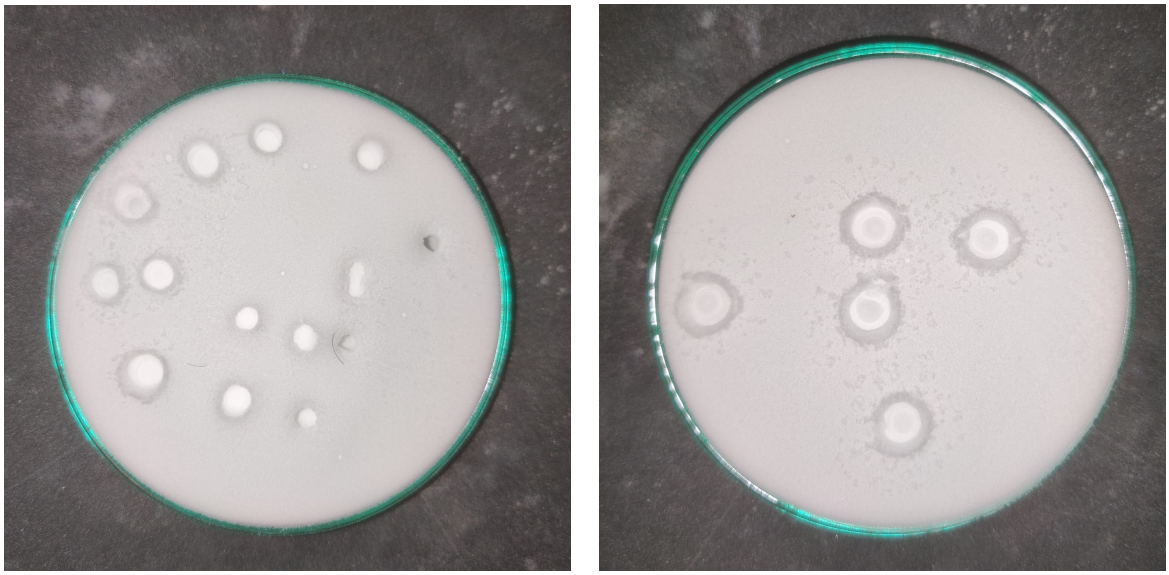

(a) Soil sample with inconsistent splash samples (packing density = 62%)

(b) Soil sample with consistent splash samples (packing density = 64%)

Figure 6.4: Both soil samples were subject to an ethanol drop of radius 1.5 mm dropped from a height of 64.5 mm. The effect of uniform packing density in obtaining a uniform distribution can be seen by comparing the two samples

6.3.4. Measuring technique

The goal of the experiments is to obtain the approximate diameters of the craters and the splash diameters formed (seen in Fig. 3.3) for multiple samples. Both parameters have been measured using a pair of vernier calipers.

6.4. Estimation of heights for drop fall

In order to observe the transfer of energy from drops to soil, we must obtain the kinetic energy that is being carried by each drop onto the soil. Since the composition has been estimated, it has been made possible to estimate the density of the liquid. The density has been estimated using the phase data provided by Strobridge *et al.* [50] and Friend *et al.* [21]. Assuming an altitude of formation of 40-10 km, the density of the mixture has been computed using the following relation

$$\rho_t = \rho_m m_m + \rho_n m_n$$

Where ρ_t is the density of the rain drop on Titan while ρ_m is the density of methane on Titan at the height of formation as inferred from Friend *et al.* [21]. ρ_n is the density of nitrogen as inferred from Strobridge *et al.* [50] while m_m and m_n are the mole fractions of methane and nitrogen respectively, as inferred from Table 2.1. The density of the rain drop liquid is estimated to be **486.24** kg/m^3.

For the composition estimated in Chapter 4, Graves *et al*. [26] estimated that a drop of radius 3.34 mm will have a velocity of 1.5 m/s at the point of contact with the ground. Now, in order to study the effects of rain drops on the soil, it is necessary to measure the impact of rain drops of different radii on the soil. Lorenz [37], published a list of velocities that they estimated for different sizes of drops hitting the ground on Titan. These values are shown in Table 6.1.

Table 6.1: Velocities of drops falling from a height of 10 km for different diameters as computed by Lorenz [37]

Diameter of drop (mm)	Velocity of falling drop (m/s)
0.1	0.044
0.2	0.121
0.3	0.198
0.4	0.271
0.5	0.341
0.75	0.499
1	0.638
1.25	0.761
1.5	0.865
2	1.065
2.5	1.232
3	1.372
4	1.587
5	1.737
6	1.84
7	1.91
8	1.957
9	1.987

This data however, has two limtations. Lorenz [37] assumed that the composition of the rain drop was purely methane, while the estimated composition in agreement with Graves *et al.* [26] is as shown in Table. 2.1, a mixture of methane and nitrogen predominantly. This brings about a change in the surface tension, density and subsequently mass of the drops. Secondly, the data shown does not estimate the velocity for a drop of diameter 6.68 mm (radius 3.34 mm). The velocity of the drops at this radius is a reference value since it is the only value provided by Graves *et al.* [26]. Therefore, the data by Lorenz [37] was interpolated in order to find out the velocity that would have been, for a drop of radius 3.34 mm, had it been computed by Lorenz [37]. Ergo, the nearest value to fit the data calculated by Lorenz [37] to the calculations made by Graves *et al.* [26] with the more accurate drop composition. The plot is shown below in Fig. 6.5

Further, the data from Lorenz [37] shows fall velocities computed for different fall heights (also called ceiling heights). These different heights were scaled such that the velocities resemble closer to the simulation results presented by Graves *et al.* [26]. The different fall velocities can be seen in Fig. 6.6.

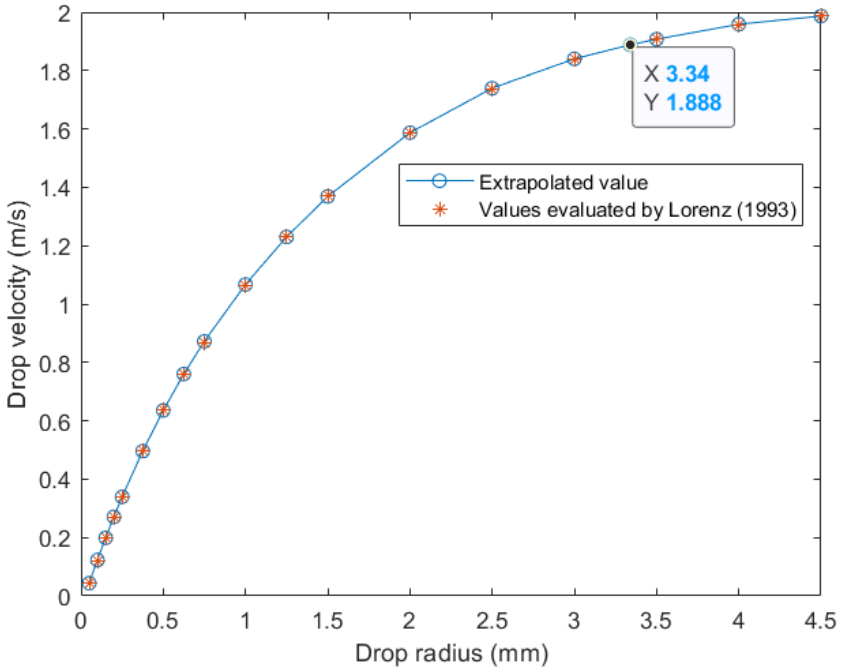

Figure 6.5: Interpolated values of velocity for varying radii. The velocity pertaining to a drop of radius 3.34 mm (diameter 6.68 mm) can be seen highlighted in this figure

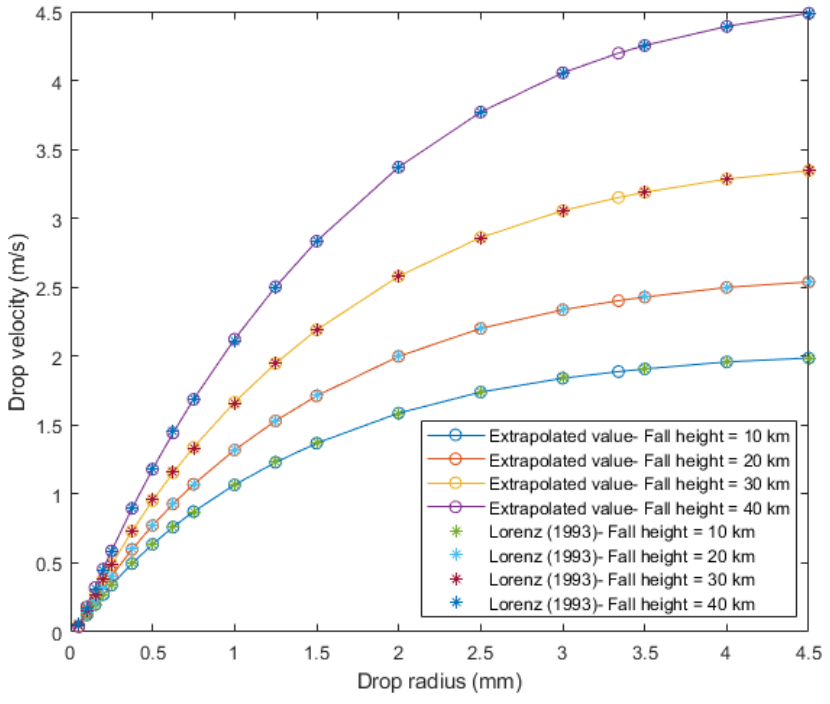

Figure 6.6: Interpolated values of drop velocity for varying radius for all ceiling heights

From Fig. 6.5, the velocity of the drop of radius 3.34 mm is determined to be 1.88 m/s. Now, this is not a very large deviation from the value calculated by Graves *et al.* [26] for a drop of same radius (1.5 m/s). Therefore, a linear scale factor can be applied to estimate the values of velocities for rain drops

of different radii as it would have been, had it been calculated by Graves *et al.* [26] This value would be 0.7978, which is the ratio of 1.5 and 1.88. This should account for the errors that were brought about by the difference in conditions in which Lorenz estimated the velocities of drops of different radii. Since the errors are accountable, it has been decided that the experiments will be carried out for all the ceiling heights that Lorenz [37]estimated fall velocities for. This means that for 3 analogs, 3 different drop sizes and 4 different fall heights, we have 12 different values of drop energies (energy remains conserved so all analogs have same energy) and 36 different fall heights and velocities. The reason for the 36 different fall heights and velocities is because while conserving energy and drop size, the different analogs with different densities have to compensate the energy and drop conservation by having different velocities with which they strike the soil sample.

Now that we have the velocities of different drops on Titan, we need to find out the energy carried by these drops. This is simple, since the kinetic energy of the drops can be found using the relation

$$K.E = \frac{1}{2}mv^2$$

Since it is kinetic energy that we aim to conserve, it is necessary to equate the kinetic energy of drops on Titan by equating them with the drops on Earth for evaluated analogs of the same radius, for a different composition (the chosen analogs don't have the same density as that of the rain drops on Titan). In doing so, the velocity of the drops for the same kinetic energy, surface tension and drop radius on Earth will be known. This is done by the following relation

$$\frac{1}{2}m_t v_t^2 = \frac{1}{2}m_e v_e^2 \tag{6.1}$$

$$m = \rho \times \frac{4}{3}\pi r^3 \tag{6.2}$$

Where m_t is the mass of drop on Titan, which can be found by the relation shown in Eq. 6.2. ρ is the density of the liquid while r is the radius of the drop. v_t is the velocity of the drops on Titan, which we recently estimated using data from Lorenz [37] and Graves *et al.* [26]. m_e is the mass of drops on Earth, which again is calculated using the same relation as shown in Eq. 6.2. In both calculations of mass of drops, the radius of the drops varies constantly (for Earth and Titan, or the left and right side of the equation) while the density changes, due to changing composition as mentioned earlier. This means that for three analogs (ethanol, n-pentane and water), 3 different sizes of drops, 4 different ceiling heights, 16 different values of kinetic energy (and therefore velocities) will be estimated.

Having calculated the velocity of drops for the relevant analogs on Earth, it is necessary to evaluate the height of fall of drops for achieving the necessary velocity via experimentation. This can simply be done using the following relation

$$h = v^2/2g \tag{6.3}$$

Where h is the height of drop that is to be computed while g is the gravitational acceleration on Earth, which is 9.8066 m/s^2. This gives rise to heights that vary with drop radii in a manner as shown in Fig. 6.7.

For varying ceiling heights, the fall heights of the drops vary for respective analog liquids, in the manner shown in Fig. 6.8.

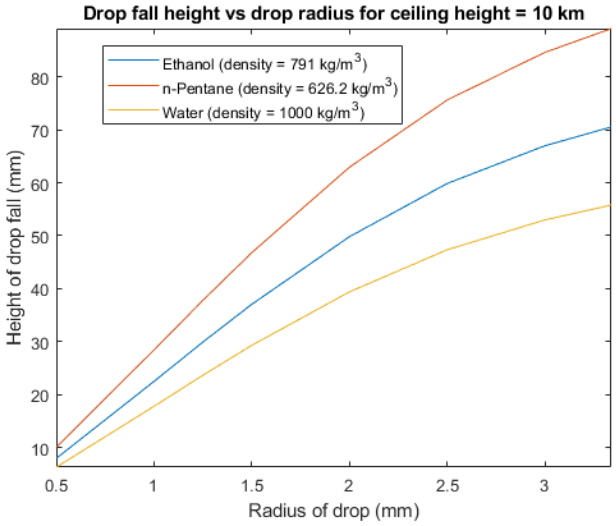

Figure 6.7: Variation of fall height with radius of drop for a ceiling height of 10 km. Drop height values have also been shown for water, for reference

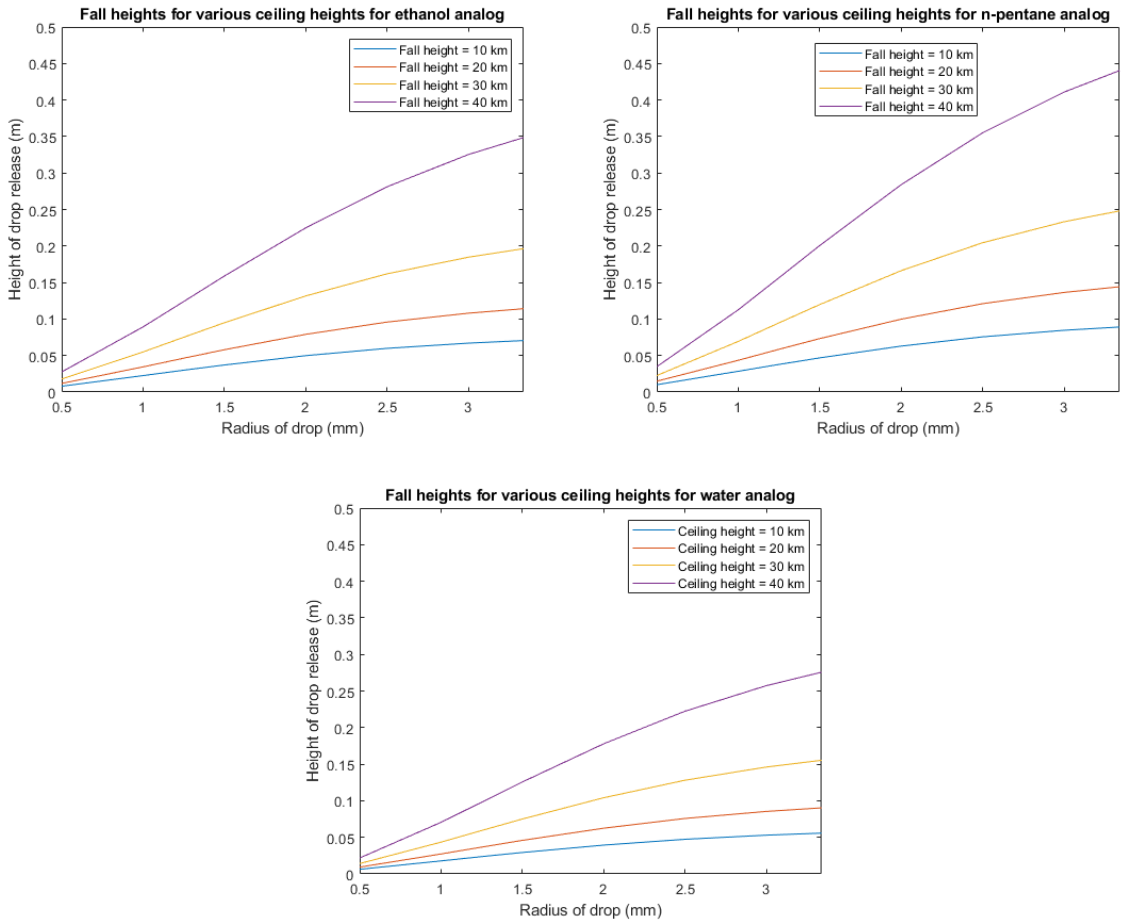

Figure 6.8: Figure showing variation of fall heights for changing ceiling heights, for each analog

6.5. Evaluation of results

In this set of experiments, a single drop of a particular analog and size will be dropped from a particular height, designated to replicate a particular ceiling height on Titan as explained above. From the experiments, two different data values will be conducted for each sample, that is generated by a single drop falling from a particular height. For a drop of particular analog, size and height of fall, 5 iterations will be conducted to ensure no unusual deviations creep into the measurements and to ensure that the sample is returning plausible measurements. This means, for 3 analogs, 4 different drop heights, 3 different sizes of drops, 5 samples per drop size, analog and height, there are 180 iterations that are executed in the extraction of data. The data that will be collected is as listed below.

1. Diameter of crater generated by splashing
2. Diameter of splash circle generated by splashing

A crater and splash circle can be visualised as shown in Fig. 3.3.

These values were averaged out for each sample. A sample is defined as a particular drop of a particular composition and drop height. Since the drop size and height are dependant, drop size is not a defining parameter for the sample. The intention was to study the characteristics of the rain drop and not the soil. There is only one kind of soil analog based on a single type of soil. Thus, the impact itself was treated as a black box.

6.5.1. Plot set 1

In this set of experiments, each sample consists of 5 iterations. Across samples, the ceiling height was varied while keeping the drop size constant. Once samples had been extracted for all ceiling heights per drop size, the drop size was then increased. This exercise was repeated until all drop sizes had been sampled, completing the quota of 180 iterations. The data collected was the diameter of the crater created by the falling drop on plain glass bubbles.

Two plots were drawn

1. Diameter of crater versus ceiling height
2. Diameter of crater versus KE of drop at moment of impact

6.5.2. Plot set 2

In this set of experiments, the nature of experiments was the same as in plot set 1. The data collected was the diameter of the splash zone around the crater created by the falling drop on plain glass bubbles.

Two plots were drawn

1. Diameter of splash circle versus ceiling height
2. Diameter of splash circle versus KE of drop at moment of impact

Across the 2 plot sets, 360 iterations were executed and 4 plots drawn. The reason for different experiment sets for crater diameter and splash circles was to reduce the risk of sample tampering, which can happen to the craters for example while measuring splash circles. Further, it also ensures that the experiments are more consistent through out all the iterations and ensures reduced deviation from desirable sample behaviour. The variation of drop fall heights with drop radius across different analogs and water is shown below in Table. 6.2. Here ceiling refers to the fall height as it would be on Titan, for a drop achieving the same velocity as it would on Earth prior to impacting the soil. The plot set 1 intended to explain the observations made on the crater formed by the splashing drop on the soil sample. All analogs had been adjusted to approximately replicate the behaviour of Titan's rain drop impacting its soil. Drop fall heights in the experiments had been calculated to obtain approximately the same velocity as a drop on Titan would on reaching the soil. Hence, it could be expected that the crater created by the splashing drop is analogous to what a drop would create on the soil of Titan. Therefore, this observation can possibly correlate directly to an observation made on Titan without further data processing.

This hypothesis cannot be extended to the splash circle diameter because the distance over which the soil particles splash is different on Earth and Titan, due to different atmospheric density at the surface and the different gravitational acceleration on both bodies. Since the splashing is occurring

on Earth, additional data processing in the form of trajectory modelling is necessary to predict how splashing of soil from the same drop with the same velocity would occur on Titan. However, being able to look at the range of splash diameters for the same ceiling heights in Earth based conditions would then later be used to put in context the splash ranges on Titan in contrast to Earth, for the same soil analog, allowing us to perceive the impact or ”performance” of each analog.

Table 6.2: Table showing the fall heights of each drop across analogs for each drop radius - input to experiments

Radius of Drop	**Scaled fall height-Ethanol (mm)**				**Scaled fall height-N-Pentane (mm)**				**Scaled fall height-Water (mm)**			
mm	Ceiling = 10 km	20 km	30 km	40 km	10 km	20 km	30 km	40 km	10 km	20 km	30 km	40 km
1	22.51	34.44	54.92	89.20	28.44	43.51	69.37	112.67	17.81	27.24	43.44	70.55
1.25	29.92	46.35	75.02	123.94	37.80	58.55	94.76	156.56	23.67	36.66	59.34	98.04
1.5	37.05	57.95	94.89	158.86	46.80	73.20	119.86	200.67	29.31	45.84	75.06	125.66

7

Particles living in a simulation

From the conducted experiments, the average height and spread of the soil bubbles will be used to evaluate the mean trajectory of the particles (two dimensional motion is a quadratic curve since displacement is proportional to the square of acceleration and linearly proportional to the initial velocity). The average kinetic energy of the bubbles will also be computed. Since the kinetic energy of the drop is already known and the number of bubbles that have been distributed can be estimated, we can find out the kinetic energy that each bubble might have received and compare that to the average kinetic energy computed from the mean values. This allows us to visualise the kinetic energy lost to particle cohesion, inter-particle collisions and liquid-particle adhesion. The ratio of the average calculated kinetic energy to kinetic energy of the drop will be the final evaluated characteristic of the drop. This will be used to evaluate the impact that n-pentane and ethanol have separately and these values will be contrasted against water to show the difference in splash erosion that rain on Titan and Earth experience that is brought about by the changing composition and gravity across the two bodies.

In order to find the energy that the particles are carrying away and to estimate the distance they are travelling, it is necessary to estimate the trajectory of the projectile. Further, visualising the trajectory of the particle serves as a proof that the built model results in an actual trajectory that the projectile is possibly taking. This means, that the initial velocity of the soil particles (which will be known due to the conservation of kinetic energy across Titan and experimental simulations) needs to be estimated from the data gathered in the analog experiments, which is the crater and the splash diameter.

For constructing this trajectory, the initial velocity of the soil particles is necessary. For estimating this, a trajectory simulation model has been built to first mimic the behaviour of the projectile upon being impacted by the drop in the experimental simulation and then, this behaviour will be exported to how the sand particles on Titan would behave. This means, that firstly, the trajectory of a particle that is being splashed from the falling drop on Earth (so a particle of the soil sample in the experiment) will be determined. Once this is done, the model will be built to factor in the conditions on Titan to predict possibly, a trajectory of a hypothetical soil particle on Titan on being impacted with a rain drop.

7.1. Building the Soil Particle Trajectory Simulation model

In order to estimate the initial velocity of a soil particle, one must factor in the forces that are influencing it on its path to reach a designated distance, which in this case, is determined by the splash and the crater diameter. The influencing forces in this case, are

1. Gravitational force of Earth
2. Drag force of atmosphere

This implies, that in this simulation, the forces of lift and wind of any kind do not influence the motion of the particle. It is also assumed that the particle is spherical in nature and moves through an atmosphere of uniform atmospheric density, temperature and pressure as that of the surface along with a uniform field of gravity. The spherical particle undergoes a purely translational motion without any sort of rotation

about its axes. The particle is assumed to be a solid glass sphere of reduced uniform density (since the experimental glass bubbles are hollow spheres) in order to correctly estimate the mass of the glass sphere. The assumed properties of the glass bubbles are taken from the catalogue and are as follows

1. Diameter of bubble: 65 μm
2. Density of bubble: 120 kg/m^3

In this scenario, the force of drag is determined by the velocity of the particle. Based on literature [36, 7, 51], the relationship between drag force and velocity of particle is given by

1. $D_f \propto V$ if $R_e < 1$. This is the Stokes regime
2. $D_f \propto V^2$ if $R_e > 1000$. This is the Newtonian regime

Where R_e is the Reynold's number of the projectile. These are two regimes of drag force. However, there is an intermediate region, referred to as the transition region, where both laws do not fully comply. The trajectory of the particles I have been attempting to estimate is not fully possible to arrive at since the initial velocities of the particles are such that they fall in the aforementioned transition region. For context, the Reynold's number R_E is given by the following equation

$$R_e = \frac{\rho v d}{\eta} \tag{7.1}$$

Here, ρ is the density of the medium in which the projectile is moving- air. The density of air is taken to be 1.2 kg/m^3. The diameter of the 2D projection of the projectile when viewed in the direction of the wind is referred to by d. Since the projectile is a sphere, this basically is the diameter of the sphere. Dynamic viscosity is η, which on the surface of Earth is 18.5 $\times$ 10^{-6} Pa-s. The velocity of the projectile, given by v, varies between and 19 m/s, all of which give rise to a value of 11.02 and 73.02 for the Reynold's number. This means that as mentioned before, the projectile motion falls in the transition regime and hence, no approximate trajectory can be constructed for the soil particle projectile- it can only be said to exist within a range, the boundaries of which are defined by the two aforementioned drag regimes, out of which models have been constructed.

7.1.1. Linear model

The model estimated follows the methodology laid out by Bernardo et al. [7] and Erlichson [20]. In this regime, as mentioned before, the force of drag is directly proportional to the velocity of the projectile moving through the medium. This means, a model to visualise drag force can be set up in the following manner

$$F_D = -kV \tag{7.2}$$

Where V is the velocity of the projectile and k is the linear drag coefficient. it is negative because the force acts in the direction opposite to the velocity vector. For this mode, Stokes [49, 14] derived an expression for the linear drag coefficient for a sphere moving through a uniform medium at rest

$$k = 6\pi\eta r \tag{7.3}$$

Here, η is the dynamic viscosity of air while r is the radius of the sphere. Using this relation, I built the model for the trajectory, the derivation for which is explained below.

Horizontal position

The drag force, as mentioned before, acts in the opposite direction to the velocity. This means both the velocity and the drag force have a certain horizontal component to it through out the flight. A free body diagram of the projectile has been drawn here in Fig. 7.1

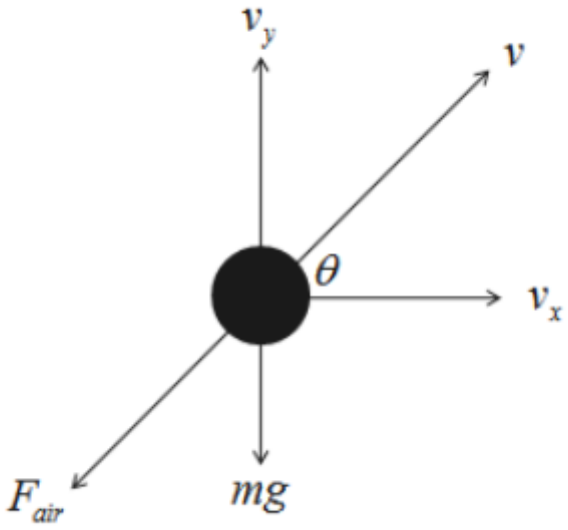

Figure 7.1: Approximate free body diagram of a freely moving body subject to drag and gravity. Here, V_x and V_y are the velocity components of the projectile in the x and y direction and F_D is the resistance force of drag acting on the projectile. Image credits: www.Bartleby.com

Balancing the horizontal forces, we have

$$\begin{aligned} F_{Dx} &= m\frac{dV_x}{dt} \\ -kV_x &= m\frac{dV_x}{dt} \\ \implies -\frac{k}{m}dt &= \frac{1}{V_x}dV_x \end{aligned}$$

Here, m is the mass of the projectile and t is the time of flight at a particular instance. Integrating t from $0 \rightarrow$ t and V_x from $V_x(t=0)$ = $V_{x0} \rightarrow V_x(t=t)$ = V_{xt}, we get

$$\begin{aligned} -\int_0^t \frac{k}{m}dt &= \int_{V_{x0}}^{V_{xt}} \frac{1}{V_x}dV_x \\ \frac{-k}{m}(t-0) &= ln\frac{V_{xt}}{V_{x0}} \\ \implies V_{xt} &= V_{x0}e^{\frac{-k}{m}t} \end{aligned} \tag{7.4}$$

This points to an exponential decay rate of the velocity of the projectile in the x direction as it traces a path through the medium. Now, to find the horizontal position, it is necessary to implement the following relations

$$\begin{aligned} V_x &= \dot{x}(t) \\ \frac{dV_x}{dt} &= \ddot{x}(t) \\ \mu &= \frac{k}{m} \end{aligned}$$

Where $x(t)$ is the position of the projectile as it varies with time t and the dots indicate the differential degree of the position function while μ is the ratio of the linear drag coefficient to the mass of the particle. Now, we have from the previous relations,

$$-kV_x = m\frac{dV_x}{dt}$$
$$\Longrightarrow \dot{x}(t) = -\frac{1}{\frac{k}{m}}\ddot{x}(t)$$

Integrate t from 0 $\rightarrow$ t. Applying limits for a particular launch angle θ, we have

1. at t = 0, $\dot{x}(0)$ = V_{x0} = $V_0 cos(\theta)$
2. at t = 0, $x(0)$ = 0
3. at t = t, $\dot{x}(t)$ = $V_x t$ = $V_{x0}e^{-\mu t}$
4. at t = t, $x(t)$ = $x(t)$

Here, V_0 is the initial velocity of the projectile. Then, on integrating and applying limits, we have

$$x(t) - 0 = \frac{-1}{\mu}(V_{x0}e^{-\mu t} - V_0 cos(\theta))$$
$$x(t) = -\frac{1}{\mu}(V_0 cos(\theta)e^{-\mu t} - V_0 cos(\theta))$$

Leading to the expression for the horizontal position, being

$$\boxed{x(t) = -\frac{1}{\mu}V_0 cos(\theta)(e^{-\mu t} - 1)} \tag{7.5}$$

Vertical position

Implementing the forces depicted in the free body diagram, on balancing, we obtain the following equation

$$-kV_y - mg = m\frac{dV_y}{dt}$$

on simplifying, we obtain

$$V_y + \frac{mg}{k} = -\frac{m}{k}\frac{dV_y}{dt}$$
$$\Longrightarrow -\mu dt = \left[\frac{1}{V_y + \frac{g}{\mu}}\right] dV_y$$

Integrating t from 0 $\rightarrow$ t and V_y from $V_y(t=0)$ = $V_{y0} \rightarrow V_y(t=t)$ = V_{yt}, we get

$$-\int_0^t \mu dt = \int_{V_{y0}}^{V_{yt}} \left[\frac{1}{V_y + \frac{g}{\mu}})\right] dV_y$$
$$\Longrightarrow -\mu(t-0) = ln\left(\frac{V_{yt} + \frac{g}{\mu}}{V_{x0} + \frac{g}{\mu}}\right)$$

Rearranging, we have

$$V_{yt} = \left(\frac{g}{\mu} + V_{y0}\right)e^{-\mu t} - \frac{g}{\mu} \tag{7.6}$$

Again, there is an exponential decay with a linear bias in the behaviour of the vertical velocity. Now, implementing relations again in order to find vertical position, we have the following relations

$$V_y = \dot{y}(t)$$
$$\frac{dV_y}{dt} = \ddot{y}(t)$$

Substituting into the previous relations, we have

$$-k\ddot{y}(t) - mg = m\ddot{y}(t)$$
$$-\dot{y}(t) - \frac{g}{\mu} = \frac{1}{\mu}\ddot{y}(t)$$

Integrate t from 0 $\rightarrow$ t. Applying limits, we have

1. at t = 0, $\dot{y}(0) = V_{y0} = V_0 sin(\theta)$
2. at t = 0, $y(0) = 0$
3. at t = t, $\dot{y}(t) = V_y t = (\frac{g}{\mu} + V_{y0})e^{-\mu t} - \frac{g}{\mu}$
4. at t = t, $y(t) = y(t)$

Integrating and applying limits, we obtain the following expression

$$y(t) = -\frac{1}{\mu}\left(\left(\frac{g}{\mu} + V_{y0}\right)e^{-\mu t} - \frac{g}{\mu} - V_{y0}\right) - \frac{gt}{\mu}$$

Rearranging, we get

$$\boxed{y(t) = \frac{1}{\mu}\left(\left(\frac{g}{\mu} + V_0 sin(\theta)\right)(1 - e^{-\mu t})\right) - \frac{gt}{\mu}} \tag{7.7}$$

Time of ascent and flight

In order to estimate the times of ascent and flight, we will implement boundary conditions to the position equations previously derived (7.5 and 7.7) and the velocity equations (7.4 and 7.6).

The time of ascent t_a is estimated with the following boundary condition
At $t = t_a, V_{yt} = 0$. From 7.6, we have

$$V_{yt} = \left(\frac{g}{\mu} + 0\right)e^{-\mu t_a} - \frac{g}{\mu}$$

Rearranging this equation, we get

$$\boxed{t_a = \frac{1}{\mu} ln\left(1 + \frac{\mu V_{y0}}{g}\right)} \tag{7.8}$$

Now, for the time of flight, we further use the following boundary conditions At $t = t_f, y(t_f) = 0$. However, at $t = 0, y(t_f) = 0$. In order to get a solution that provides a tangible value for the time of flight, the solution to $y(t) = 0$ should be such that $t \neq 0$. Implementing the condition in Eq. 7.7, we obtain the following

$$0 = \frac{1}{\mu}\left(\left(\frac{g}{\mu} + V_0 sin(\theta)\right)(1 - e^{-\mu t_f})\right) - \frac{gt_f}{\mu}$$

$$\implies t_f = \frac{1}{\mu}\left(1 + \frac{\mu V_0 sin(\theta)}{g}\right) - \frac{1}{\mu}\left(1 + \frac{\mu V_0 sin(\theta)}{g}\right)e^{-\mu t_f}$$

In order to solve the equation such that the t_f term on the 2nd term in the RHS disappears, Bernardo et al. [7] made use of the Lambert function, the nature of which is to solve equations of the following types

$$y = xe^x \implies x = W(y)$$

Using this, they arrived at a relation for the time of flight, which is

$$\boxed{t_f = \frac{1}{\mu}\left(1 + \frac{\mu V_0 sin(\theta)}{g}\right) - \frac{1}{\mu}W\left(-\left(1 + \frac{\mu V_0 sin(\theta)}{g}\right)\right)e^{-(1 + \frac{\mu V_0 sin(\theta)}{g})}} \tag{7.9}$$

7.1.2. Quadratic model

In this regime, as mentioned before, the force of drag is directly proportional to the square of velocity of the projectile moving through the medium. Thus, a model to visualise the drag force can be setup in the following manner.

$$F_D = -k_q V^2$$

Unlike the linear models, there exists no analytical models for estimating the trajectory of a body subject to quadratic drag force. In order to estimate the drag force, it is necessary to perform integral propagation, similar to a CFD simulation. However, building such a library of forces for the Titanian

atmosphere is outside the scope of this thesis and is very time consuming. Therefore, it is not possible in this thesis to construct the trajectory of the projectile under quadratic drag. However, analytical approximations defined by Chudinov [12, 13, 11] have been useful in determining the ranges, initial velocity and time of flight of the projectile.

For a launch angle θ, coefficient of drag C_D, density of medium in which projectile is moving ρ, projected surface area against drag S, mass of projectile m moving in a constant gravitational field with acceleration g, the proportionality coefficient is defined by the following relation

$$k_q = \frac{\rho C_D S}{2mg} \tag{7.10}$$

For an initial velocity V_0 and launch angle θ, the maximum height attained for a projectile subject to quadratic drag is given by the following relation

$$H = \frac{V_0^2 sin^2(\theta)}{g(2 + kV_0^2 sin(\theta))} \tag{7.11}$$

Having established the maximum height, it is now possible to calculate the approximate time of flight using the following relation

$$T = 2\sqrt{\frac{2H}{g}} \tag{7.12}$$

In order to calculate the range of projectile flight, Chudinov [12, 13, 11] made use of the velocity of the projectile at the apex. He obtained this value using the relation mentioned below.

$$V_a = \frac{V_0 cos(\theta)}{\sqrt{1 + kV_0^2 \left(sin(\theta) + cos^2(\theta) ln(tan\left(\frac{\theta}{2} + \frac{\pi}{4}\right)\right)}} \tag{7.13}$$

Now, it is possible to calculate the range of flight of the projectile, using the following relation

$$R = V_a T \tag{7.14}$$

Using these relations, a model can be built to explain the behaviour of the projectile subject to quadratic drag. It is necessary to estimate the energy carried away by the particle so using these relations, the initial velocity needs to be determined for a particle of assumed mass and launch angle.

For both models, the initial velocity is not available. However, the ranges are available in the form of splash diameters. Particles are approximately scattered within this range all the way from the crater edge till the splash diameter. Thus, to estimate the possible initial velocities of particles that have scattered to a distance lesser than the splash radius, the splash radius is divided into 10 segments of equal distance. The distance of the end of each segment from the center is assumed to be the flight range. Using this value, the initial velocity is calculated iteratively. This means, that for each flight range, the initial velocity is initially assumed to be 0.01 m/s and the trajectory is computed. If the calculated trajectory for the trajectory does not equal the flight range of that particular segment, then the velocity is incremented by 0.001 m/s. This is repeated until the trajectory parameters are fulfilled, meaning that an initial velocity that gives rise to a range that is closest to the actual flight range of the segment is obtained. Of course, during the process, other parameters are also calculated. These are, the maximum height of the projectile and the time of flight of the projectile. At the ”agreeable” value of initial velocity, these terms are also assumed to be correct since they are in agreement with the model that has been established. This calculation has been executed on Matlab and the code is also made available as such. The validation for these models have also been executed and have been shown below.

7.1.3. Behaviour of a soil particle on Titan

Since the experiments were performed using analogs, the drop soil interaction is nearly accurate in terms of splash initiation and energy transfer between soil and drop. However, the splashing particles move through different mediums on Earth and on Titan. The change in atmosphere and the different gravity will obviously result in different trajectories and consequentially, different splash diameters.

Furthermore, the size and density of soil particles on Titan are supposedly different and the values obtained in literature [61, 9] have been implemented for understanding their behaviour. In order to visualise these trajectories, the parameters that are again required to be translated from Earth to Titan so that the same model that has been outlined previously may be implemented, are listed below.

1. Change in acceleration due to gravity at the surface to Titan (1.354 $\mathrm{m/s}$ [54]) from Earth (9.8066 $\mathrm{m/s}$)
2. Changing atmospheric density at surface to Titan (5.28 $\mathrm{kg/m^3}$ [15]) from Earth (1.2 $\mathrm{kg/m^3}$)
3. Changing dynamic viscosity of atmosphere to Titan (6.028×10^{-6} Pa $-$ s) from Earth (18.5×10^{-6} Pa-s)

The dynamic viscosity on Titan was calculated using the following relation between viscosity and temperature [23, 8]

$$\eta = 1.8325 \times 10^{-5} \left[\frac{416.6}{T + 120}\right] \left[\frac{T}{296.16}\right]^{\frac{3}{2}} \quad \mathrm{kgm^{-1}s^{-1}} \tag{7.15}$$

Where η is the dynamic viscosity, T is the absolute temperature of the atmosphere. For a value of 90 K [26] at the surface, we obtain a value of dynamic viscosity that is

$$\eta = 6.038 \times 10^{-6} \quad \mathrm{kgm^{-1}s^{-1}} \tag{7.16}$$

Using these values, possible trajectories were constructed using both linear and quadratic models for Titan for a median splash distance (half the maximum possible splash range to visualise an average particle's behaviour). They are shown below for different drop sizes.

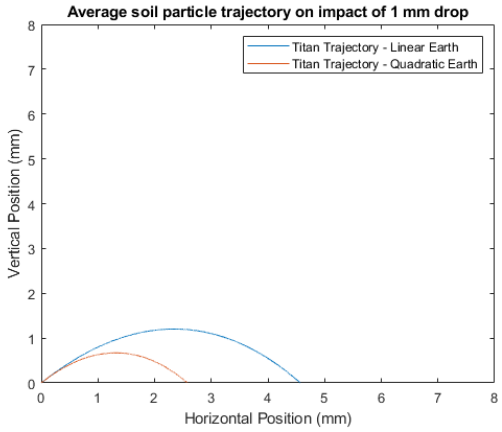

(a) Drop radius = 1 mm

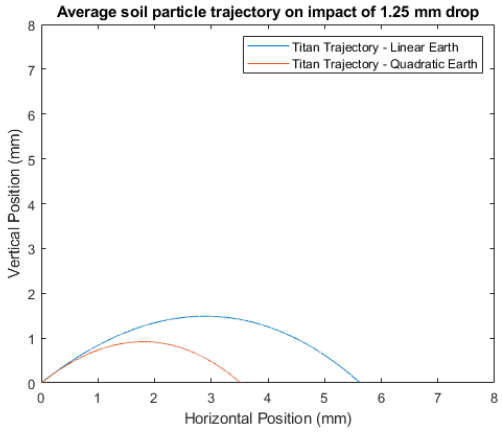

(b) Drop radius = 1.25 mm

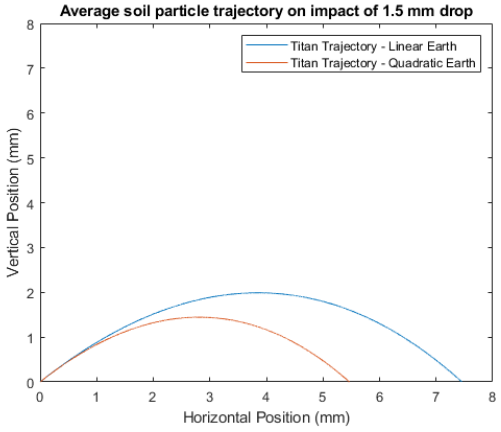

(c) Drop radius = 1.5 mm

Figure 7.2: Possible trajectories visualised for both models for varying drop sizes, derived from energy calculations for ethanol analog

7.2. Building the Drop Energy Split Simulation model

This model is built to simulate and predict the mass of soil being carried away due to the impact of a splashing drop. This mass in turn will make it easy to estimate the amount of energy being carried away totally by the splashing particles since the Soil Particle Trajectory Simulation model has made it possible to estimate the mass that a single particle traversing a particular range is travelling.

Due to the existing soil splash erosion studies carried out on Earth, Van Dijk *et al.* [19] developed a model that was later improved by Leguedois *et al.* [34] and then by Mouzai *et al.* [40]. This model is explained subsequently.

Van Dijk *et al.* [19] describe the mass of soil splashing at a one dimensional point m_{point} using an equation they refer to as the fundamental splash distribution function (FDFS) since this is the equation from which all subsequent equations are derived from. This is mentioned below

$$m_{point} = \frac{\mu}{\Lambda 2\pi r} e^{-\frac{r}{\Lambda}} \tag{7.17}$$

Here, μ is the rate of soil detachment (g/m^2), Λ is the average splash length, that is, the mass weighted average radial distance over which the particles are splashed. It is mentioned however, that the highest density of splashed particles will occur around the crater perimeter [19] and therefore it makes sense to use the crater diameter as the average splash length. Hence, the value of Λ is obtained from the observations made in the experiments, and is the value of the crater diameter. To clarify, this is the crater diameter obtained from the experimental observations. This is because the drop impact itself is considered a black box in this thesis. Hence, the nature of the impact is relatively constant, whether it is in a lab on Earth or is actually happening on Titan since the usage of analogs is helping recreate the nature of drop impact on Titan's soil on Earth. Now to estimate the amount of soil mass splashed in a two dimensional ring M_{ring} in the splash zone, the following expression is used.

$$M_{ring}(r) = 2\pi r m_{point}(r) = \frac{\mu}{\Lambda} e^{-\frac{r}{\Lambda}} \tag{7.18}$$

This is an analytical approximation that is multiplying a single point over the length of the perimeter of a ring at a particular radius r. Now, in order to obtain the mass of the splashed particles through out the entire splash zone, which is given by the following expression

$$M = \int_{R_c}^{R_s} M_{ring} dr$$

Where R_c is the radius of the crater and R_s is the radius of the splash circle. Van Dijk *et al.* [19], make use of an analytical approximation to this expression

$$M_{splash} = a \int_0^{\infty} M_{ring} dr = a\mu \tag{7.19}$$

Where a is the area of the splash zone. Therein, lies the model. Now in order to implement the model, it is first necessary to establish the value of μ, or the rate of soil detachment. In order to determine this parameter, Mouzai *et al.* [40] provided an empirical relation correlating the rate of soil detachment to the shear strength of the soil. This relation is given by

$$\mu = -4 \times 10^{-7}\tau^2 - 10^{-6}\tau + 0.32 \tag{7.20}$$

Here, τ is the shear strength of the soil surface in kPa. Now, shear strength of the soil needs to be obtained. The compressive strength of the soil analog is mentioned in the technical documentation of the glass bubbles [1]. Using Cauchy's criterion for pseudo solids in a network that are bound together by a cohesive force (akin to multiple particles such as glass bubbles packed together in a sample), the ratio of compressive or bulk modulus to shear modulus is given by the following boundary relation.

$$K/G = 5/3 \tag{7.21}$$

Here, K is the bulk modulus while G is the shear modulus. Since it is assumed that force is translated unilaterally in all directions and that the glass bubble behaves as an isotropic body, the ratio has been applied to the compressive strength and the shear strength of the material, making it possible to obtain the shear strength of the bubbles. Once the shear strength is obtained, the rate of detachability is obtained and subsequently, the displaced mass of the splashing particles. From this, the energy of the splashing particles is obtained using the following relation.

$$E_{splash} = \frac{M_{splash} E_{SBP}}{2M_{particle}} \tag{7.22}$$

Now, E_{SBP} is the energy of the Splash Boundary Particle (SBP), meaning that this value correlates to the energy of a particle traveling all the way to the boundary of the particle. M_{splash} is the mass of the splashed particles, $M_{particle}$ is the mass of a single splashing particle. The ratio of M_{splash} to $M_{particle}$, when multiplied by E_{SBP} would give us the energy of all particles had they all been transported to the splash boundary. However, most of the particles do not travel to the splash boundary and fall much more within that range. Therefore, the product is divided by 2, meaning the average of the total SBP energy has been calculated to obtain an approximate value of the average energy of all particles put together.

8

Models being validated

In this chapter, the validation for the models that have been constructed will be provided.

8.1. Validation for the Soil Particle Trajectory Simulation Model

The validation for both models was performed based on different sources in literature. They are further described below

Linear model

The validation for the linear models has been done using the cases outlined by Erlichson [20]. The paper covers the situation of a flying golf ball that has been hit at differing initial angles. The trajectory is from the moment the ball, at rest, is hit from the ground till the moment it first lands on the ground again. For this, the assumed parameters are as follows.

1. Initial velocity V_0 = 60.96 m/s (200 ft/s)
2. Angle of launch θ = 10° - 50°
3. Drag coefficient to mass ratio $\mu(= k/m)$ = 0.25, 0.5 s^{-1}

For the different values of μ, Erlichson [20] produced two different ranges of trajectories for the different angles of launch, These trajectories are shown below in 8.1 and 8.2

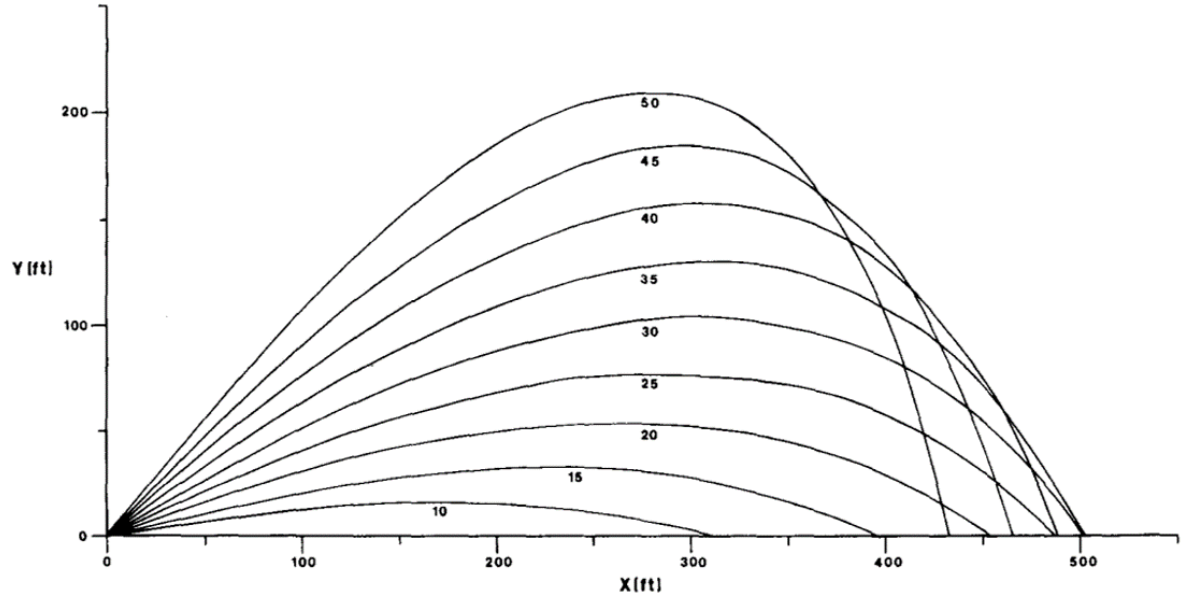

Figure 8.1: Range of trajectories for μ = 0.25 s^{-1}

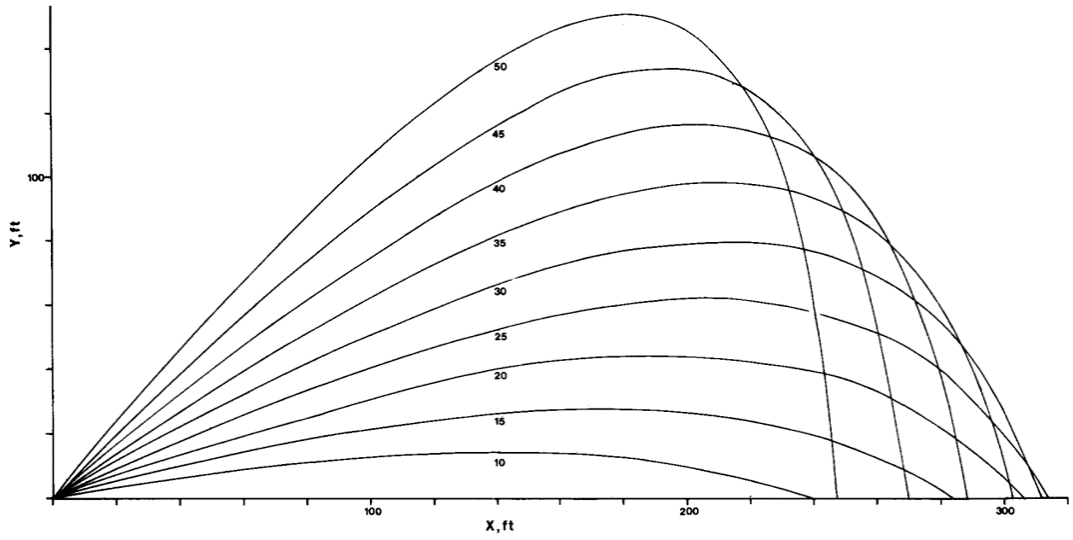

Figure 8.2: Range of trajectories for μ = 0.5 s^{-1}

The validation for these trajectories is shown below in Fig. 8.3 and Fig. 8.4. These trajectories have also been constructed on Matlab and the codes for the same have been made available.

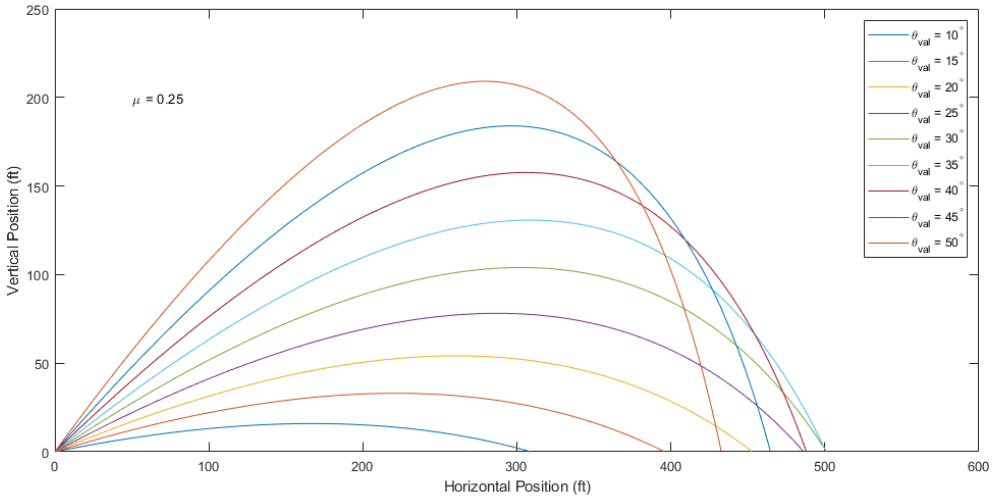

Figure 8.3: Validation trajectories for μ = 0.25 s^{-1}

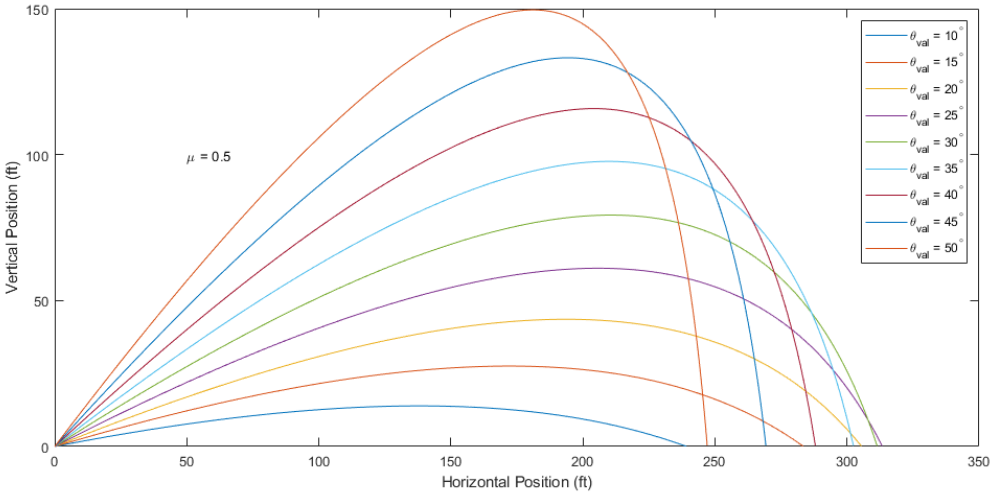

Figure 8.4: Validation trajectories for μ = 0.5 s^{-1}

Since the computed trajectories have been achieved using the same model and appear to be a faithful recreation of the trajectories laid down by Erlichson [20], the model is considered validated and truthful to particle trajectory behaviour as described by literature.

Quadratic model

For the quadratic model, the values of maximum height, range etc. laid out for the case detailed by Chudinov [12]. The case attempts to study the behaviour of a flying baseball that has been initiated in its trajectory with the following initial values.

1. Initial velocity V_0 = 40m/s
2. Launch angle θ = 45°
3. Drag proportionality constant k = 0.000625 s^2/m^2
4. Acceleration due to gravity = 9.81 m/s^2

For these initial values, the obtained output as generated by Chudinov [12] and by using the model constructed on Matlab are contrasted below

Table 8.1: Validation of the results generated by Chudinov [12] for the model used to visualise the behaviour of a moving projectile subject to quadratic drag

Parameter	Literature value	Model output
Maximum height H (m)	30.1	30.1242
Time of flight T (s)	4.96	4.9564
Apex velocity V_a (m/s)	19.3	19.2996
Flight range (m)	95.7	95.6571

8.2. Validation for the Drop Energy Split Simulation model

There exists no numerical validation for this model. This is because the FDFS function was derived as an empirical approximation that was tested on well sorted sediment (silt loam, silt clay loam and clay loam) [47] and on 9 types of loose soil [44] by Van Dijk *et al.* [19]. This validation was further extended to bulk aggregated soils and aggregate size fractions (0.05 μm $\sim$ 2000 mum) for the aforementioned well sorted sediment by Leguedois *et al.* [34]. It was understood that since the model could approximately accommodate the behaviour of splashing soil of various kinds and across different grain sizes, the model could be implemented for predicting the behaviour of Titan's soil as well. The applicability of this model to Titan's soil can only be tested in the future when there is more information gathered on Titan's soil and due to limitation of information, lies beyond the scope of this thesis.

9

A discussion on everything that resulted

The data collected from the experiments were sufficient enough to justify drop-soil interaction to the extent of the crater diameter, since the analog transition implies that the assumption of the glass bubble sample's behaviour akin to Titan's soil is valid. However, the splash diameter is a different value in the lab and on Titan, owing to the different atmospheric densities at the surface on Earth and Titan. This justified the building of a model that predicted the supposed trajectory of the soil particle analog, which was later extended to explain an approximate behaviour of an actual soil particle on Titan. This is not enough, since the goal was to determine the amount of energy the collective splashed particles were carrying away. In order to determine this energy, it was necessary to determine first, the approximate mass of particles that were being splashed away. For this, another model was built, that relied on both the splash circle diameters and the trajectory model. Both models put together, build a complete picture of the approximate behaviour of all splashed particles. Both the models have been explained in Chapter 7. A visual representation of this workflow is shown below in Fig. 9.1. Now, all relevant results; from experimental observations and those brought about by computing both models will be explained in this chapter.

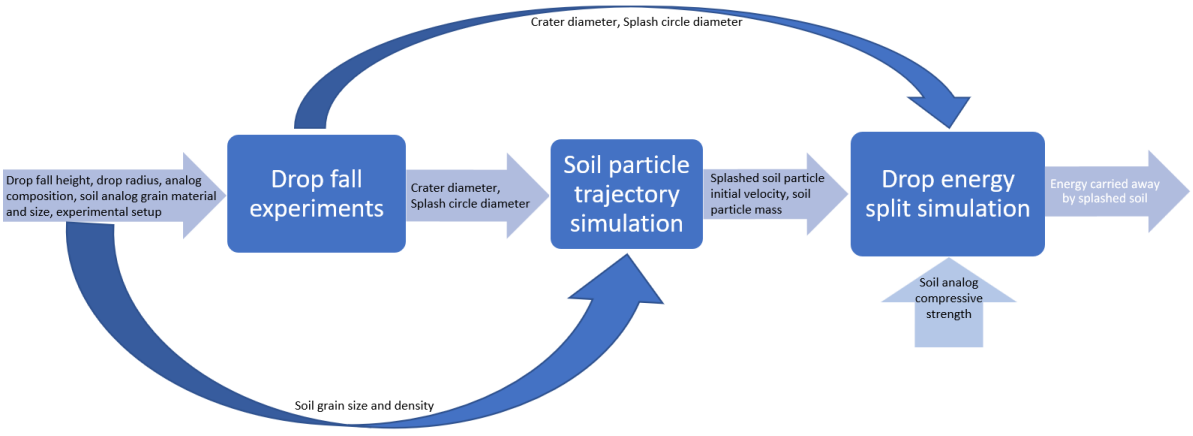

Figure 9.1: Flowchart of work with inputs and outcomes from different activities and the final result

9.1. Experimental observations

It was mentioned in Chapter 6 that there would be two plot sets for each different sets of experiments, meaning there would totally be 4 different kinds of plots for a drop of particular radius, comparing different analogs to put into context how each analog impacted the soil compared to water. They are shown below

9.1.1. Plot set 1

Diameter of crater versus ceiling height

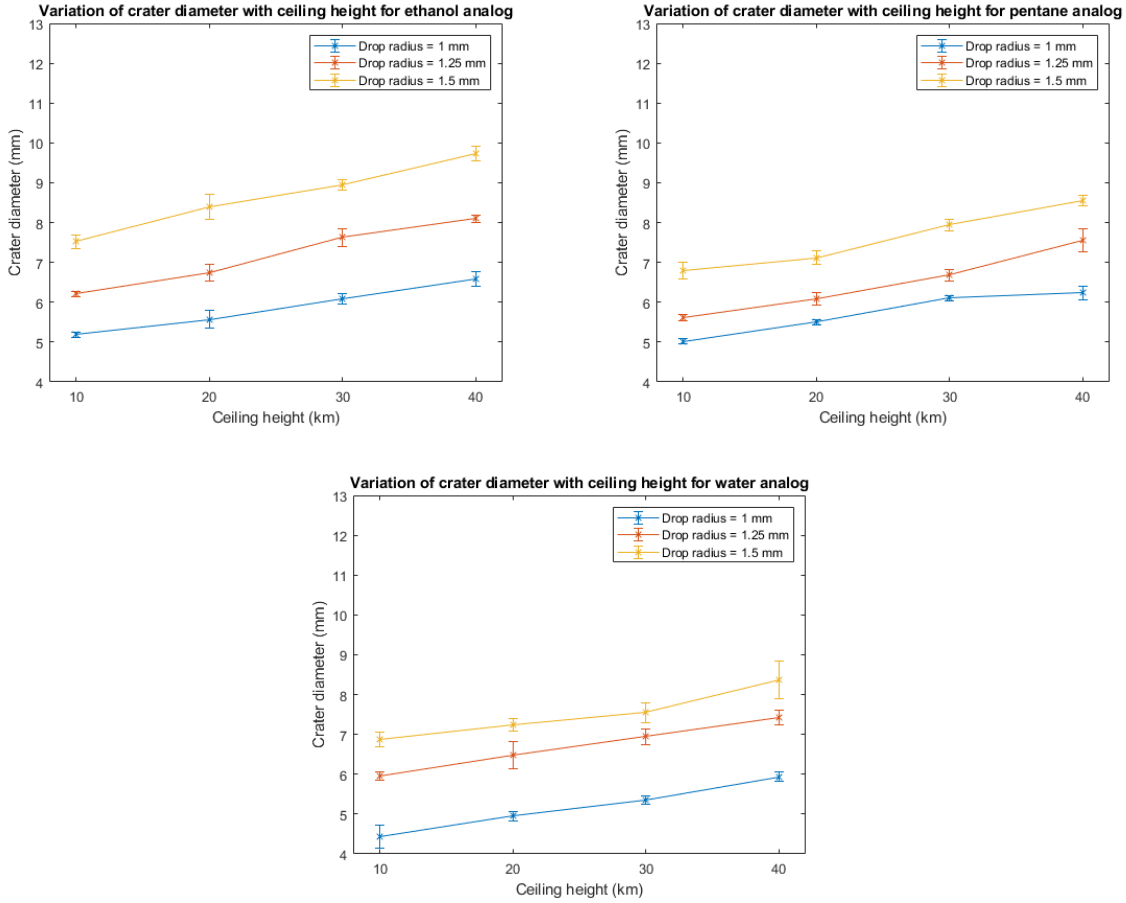

Figure 9.2: Variation of crater diameter with ceiling height for different analogs and water. It can be seen here that the diameters produced by the two analogs are similar to the diameters produced by splashing water. All plots are scaled equally

An immediately noticeable feature of this plot is that there appears to be a (nearly) linear relation between the ceiling height and the crater diameter. There appears to be not much difference in the diameters created by either of the analogs and water. There is a slight increase in crater diameters produced by both analogs compared to water for a drop radius of 1 mm but as the drop size increases, the difference is not very much pronounced. This could imply that surface tension does not influence the formation of drop craters for the soil on Titan.

Diameter of crater versus drop kinetic energy

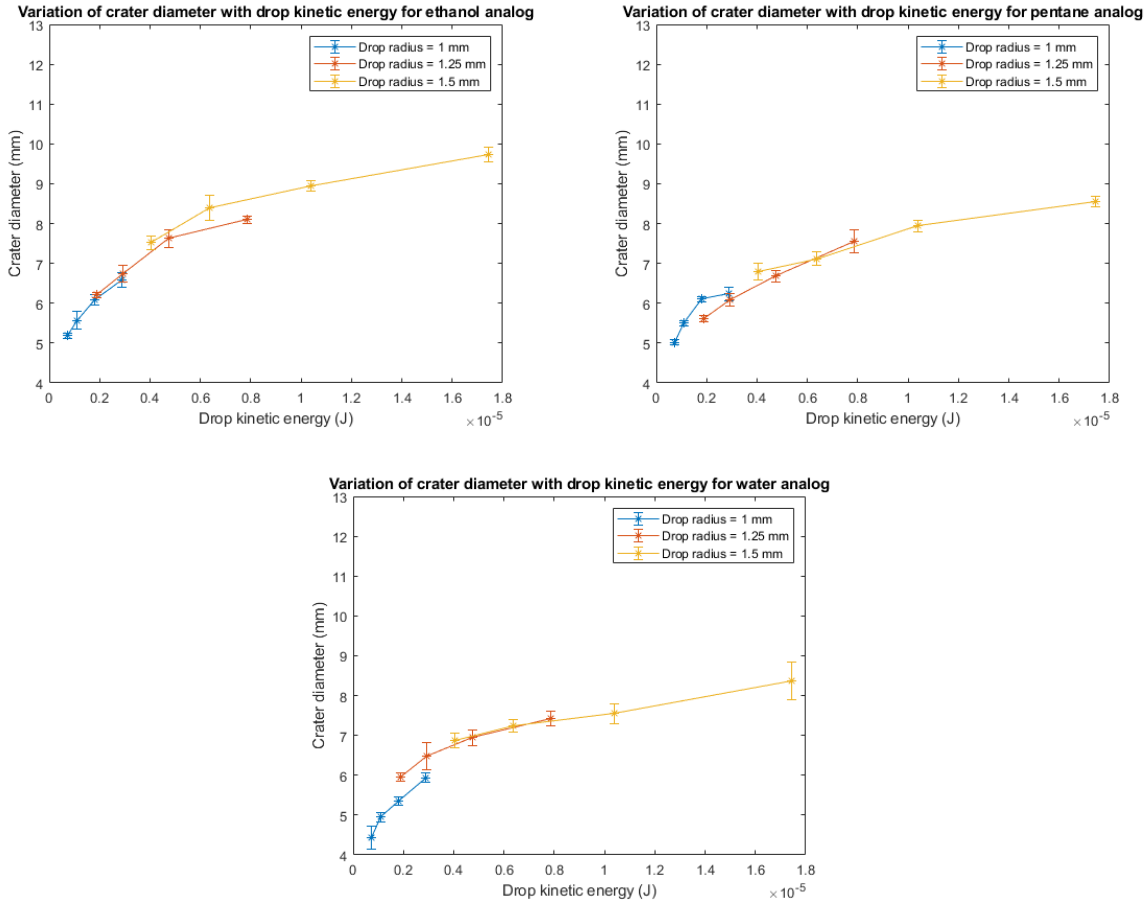

Figure 9.3: Variation of crater diameter with drop kinetic energy for different analogs and water. All plots are scaled equally

Unlike the ceiling height, there appears to not be a linear relation between the crater diameter and the drop kinetic energy. The curve appears to be intuitive because there is a linear relation between the drop fall velocity and the crater diameter (plots can be found in Appendix B).

9.1.2. Plot set 2

Diameter of splash circle versus ceiling height

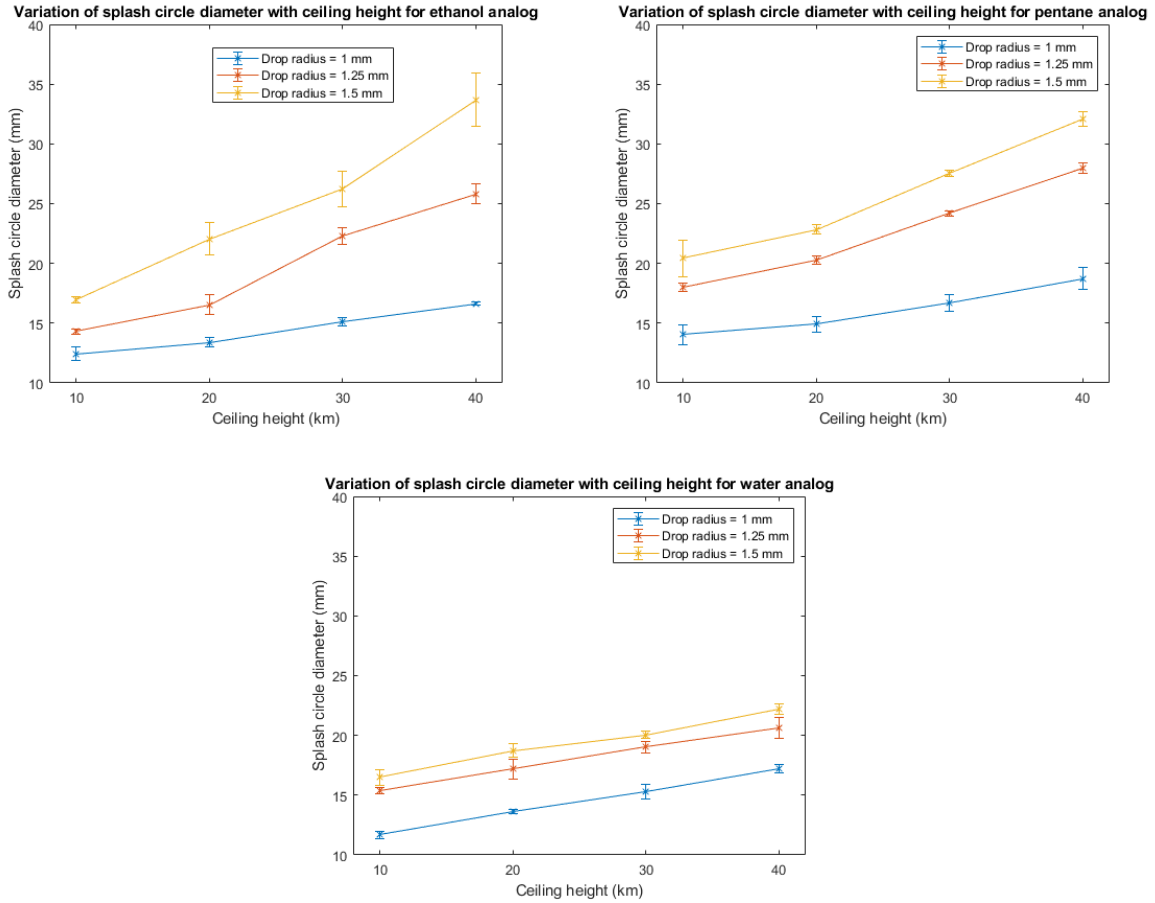

Figure 9.4: Variation of splash circle diameter with ceiling height for different analogs and water. It can be seen here that the diameters produced by the two analogs are distinctly higher than the diameters produced by splashing water for increasing drop sizes. All plots are scaled equally

Unlike the crater diameter, there appears to be an increasing value of splash circle diameter with increasing drop size. This could mean that at higher drop sizes, there is a greater percentage of energy being transferred from the drop to the soil particles that are being splashed. This could be because of the lower cohesive forces that bind the drop molecules together in the two analogs.

Diameter of splash circle versus drop kinetic energy

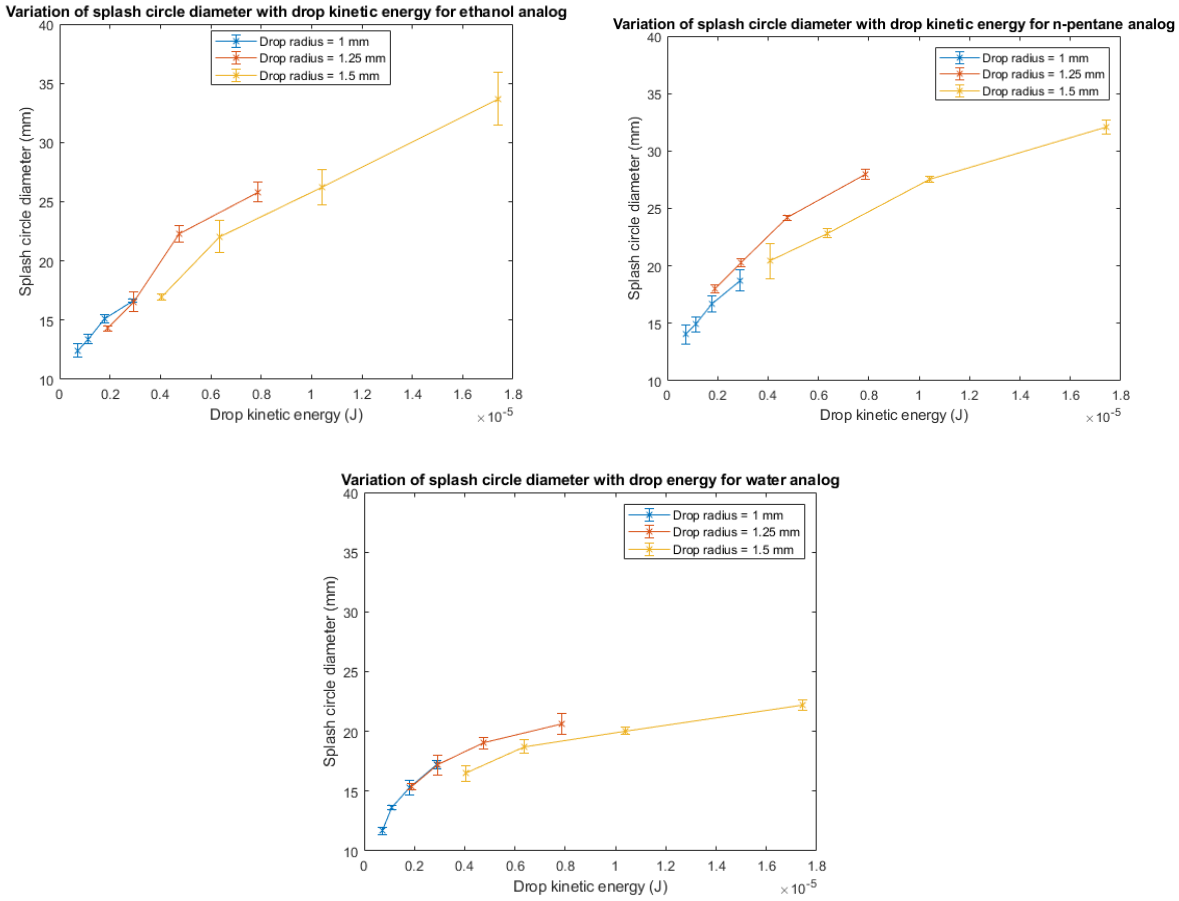

Figure 9.5: Variation of splash circle diameter with drop kinetic energy for different analogs and water. All plots are scaled equally

It can be seen from these plots that for the same drop energy, the splash circle diameter recorded is much higher for ethanol and n-pentane compared to water (especially at higher drop sizes). This serves as better proof for the earlier hypothesis that the splashing particles are carrying away more energy from the analog drops in comparison to water, for the reasons mentioned above. This has to be a plausible explanation to justify the additional distances travelled by the soil particles.

9.2. Trajectory modelling

In this section, the approximate trajectories of soil particles on Titan are explained. But in order to do this, the trajectory model first needs to predict the trajectory of the soil particle analogs- the glass bubble for the experimental simulations conducted on Earth. This is necessary because the data extracted from the experiments - the splash circle diameter forms the input for determining the trajectory as mentioned in Chapter 7. Using this, the initial velocities of the particles being splashed can be estimated. These initial velocities help determine the trajectory on Titan as well.

It was observed for the Earth based analogs, that the initial velocities born by the particles implied that they moved through the air at a recorded Reynold's number R_e falling in the range of 8.303 - 1801.621. This means that neither the linear (valid for $R_e < 1$) nor the quadratic model (valid for $R_e > 1000$) can fully approximate the trajectories of all the glass bubbles within all splash circles. This means that the 2 models will be used and we will assume that the results (the initial velocity of the splashing particles) are ranging between the results provided by these 2 models. These two values

resulting from the two models will then be used to calculate the flight ranges on Titan. On executing the models, certain trajectory ranges were obtained for the initial velocities calculated for both analogs.

To summarise the plots- Each figure set pertains to the splashing of a supposed soil particle on Titan after having been subject to drop impact. Each particle represents the mean distance traversed by all the splashed particles - the maximum possible distance of the particles travelled is twice the shown range, but is not representative of all the particles. The trajectories have been obtained using the linear model since the model provides trajectories for all particle ranges that represent expect-able trajectories of particles. The reason why the quadratic model has not been implemented to predict behaviour of soil particles on Titan is explained in the following section.

The plots produced per drop size, analog and fall height are many such that they have been shown in the Appendix A. Among the four plots in each figure set, the drop size remains the same, while the height at which it falls from increases gradually from 10 to 40 km. Subsequent plot sets have increased size of drops (kept constant through out the set again). While the initial velocities produced by both analogs record different initial velocities, the expected range of soil particle velocities remains very similar. Furthermore, a consistent behaviour that can be observed with increasing ceiling height is the fact that the range of distances travelled (defined by the area bound by the linear and quadratic model trajectories) increases, leading to increased uncertainty on how far the projectiles will travel. However, it definitely increases with increasing ceiling height, which is intuitive at first glance because drops falling from greater heights possess greater kinetic energy at the time of impact. However, the increase in flight range with fall height is not monotonous but arbitrary. For example, Fig. 9.6 shows the estimated trajectory range for an average soil particle splashed due to a drop of radius 1.5 mm falling from a height of 10 km on Titan. The drop liquid analog used to obtain the splash diameters for the models is n-Pentane in this particular case.

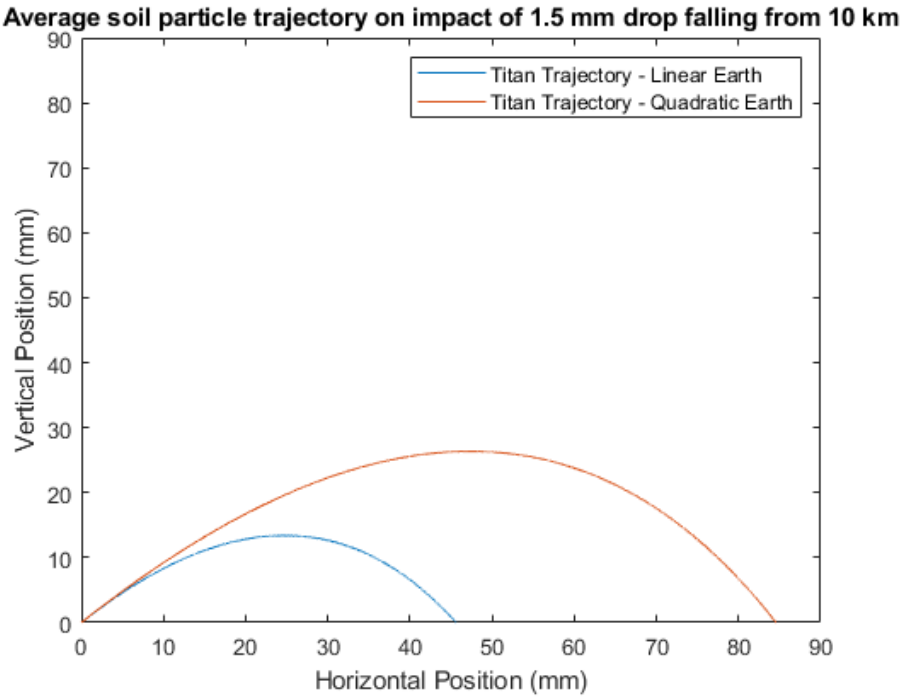

Figure 9.6: Estimated trajectory range of an average soil particle splashing due to a drop of radius 1.5 mm falling from a height of 10 km on Titan

9.3. Energy ratio plots

Using the initial velocities that were calculated using the Soil particle trajectory simulation, the Drop energy split simulation model was implemented to find out firstly, the mass of splashing particles and subsequently, the energy carried away by the splashed particles. The value of calculated energy can

be put into perspective by calculating the ratio of the energy of the splashed particles to the energy of the drop. This has been used as a performance metric of each analog to compare and estimate how much energy is being carried away by the soil with perspective of how effective water is on the same soil. It is understood that that metric will help understand where the erosive capabilities on Titan stand in comparison to Earth. The splash energies calculated using the initial velocities obtained from both, the linear and quadratic model have been contrasted with the drop energies and the plots comparing all analogs are shown below in Fig. 9.7, 9.8 and 9.9.

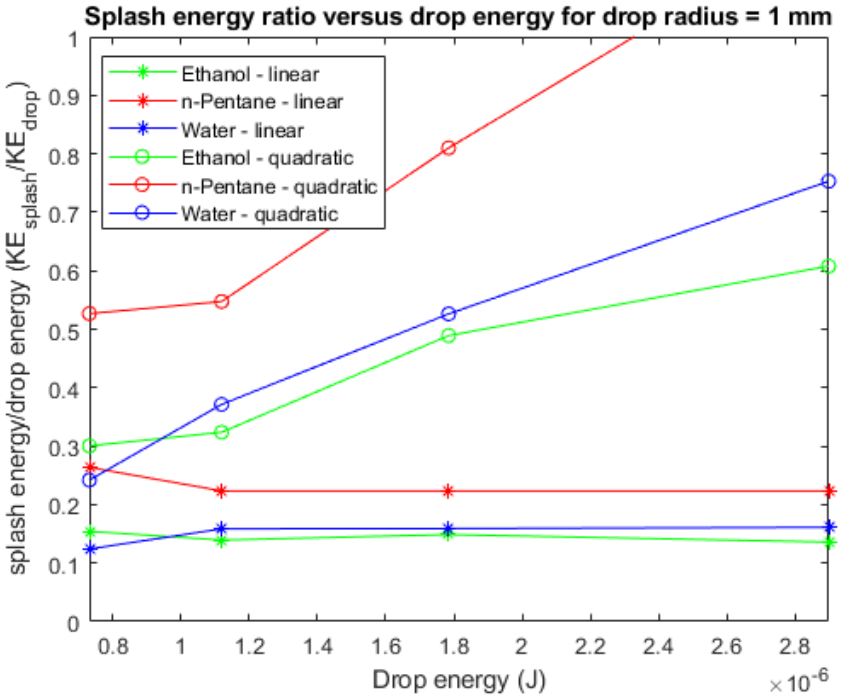

Figure 9.7: Comparison of analog performance for ratio of splash to drop energy vs drop energy for drop of radius 1 mm

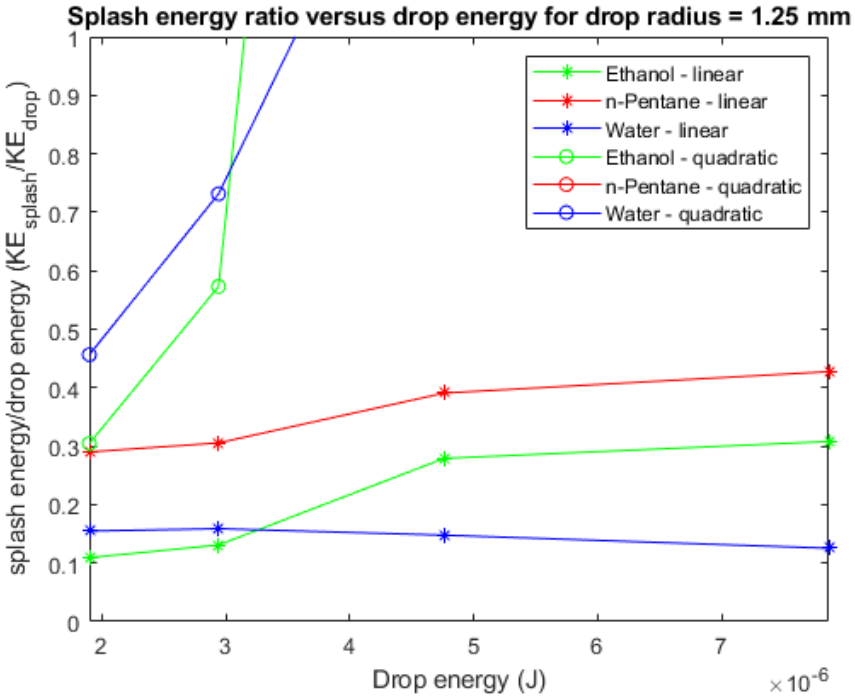

Figure 9.8: Comparison of analog performance for ratio of splash to drop energy vs drop energy for drop of radius 1.25 mm

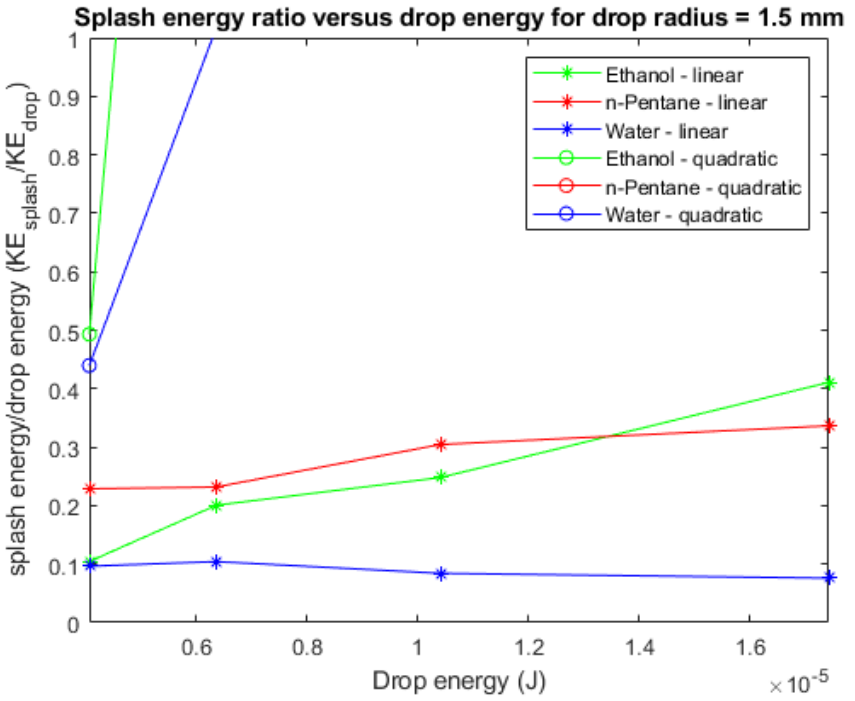

Figure 9.9: Comparison of analog performance for ratio of splash to drop energy vs drop energy for drop of radius 1.5 mm

As can be noticed, all plots are limited to a splash ratio of 1.0 on the y axis since any value that exceeds 1.0 for the ratio of splash to drop energy is incorrect, since it violates the law of conservation of energy (the energy carried away by the splashing particles put together can never exceed the energy

of the drop, that impacted with the splashing particles in the first place). It can be observed that with increasing drop size, the quadratic models for various analogs exceeds 1.0, limiting the values that are coherent. However, the curves defined by the initial velocities obtained from the linear and quadratic models form the boundaries of what is possibly the actual trajectory of the actual energy being carried away by all soil particles.

It can also be seen that the energies transferred to the soil from the analogs is comparable to water for low drop energies (fall heights) but on increasing the fall height, there is a substantial increase in the energy imparted to the soil particles from the analogs in comparison to water. This can be explained by the fact that the surface tension (and hence, the cohesive forces within the molecules of the liquid drop) of the analogs is much lower (16 mN/m for n-Pentane and 21 mN/m for ethanol compared to 71 mN/m for water), meaning that the analog drops are easily broken apart compared to water. Therefore, they should be able to impart a greater amount of their energy to the soil particles compared to water.

An increased ratio of energy transfer must translate to an increased splash range as well, since more particle energy should imply higher initial velocity, which in turn should assure an increased range of particle trajectories. The range of particle trajectories for each analog inferred measurements are shown in Fig. 9.10a and Fig. 9.10b. To clarify, the splash ranges shown for the respective analog are obtained after processing the data through both the models and obtaining an approximate extent of splash ranges for the initial velocities obtained from the **linear** model used for trajectory modelling. This is compared to the splash diameters obtained from experimentation using water as the drop on Earth, meaning the splash ranges values for the water analog are subject to **Earth conditions**. This plot set simply aims to compare the performance of the two analogs on their respective celestial body. It must be kept in mind that the shaded areas are intended to show the extent of possible splash ranges computed for each analog, had it been the rain drop on Titan, compared to the extent of splash ranges that were obtained by water on soil analog in earth based conditions. The lines in both case form an upper boundary that has been obtained using the linear model for trajectory modelling.

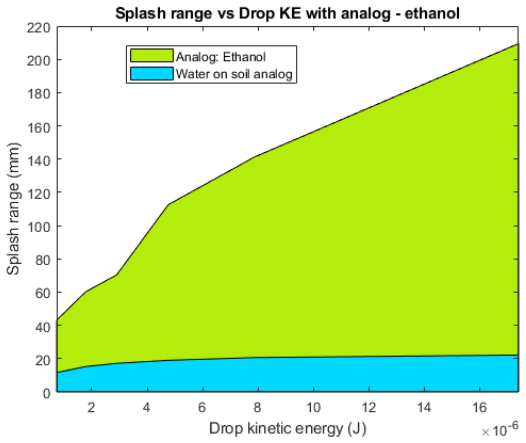

(a) Measurements made using ethanol as the analog

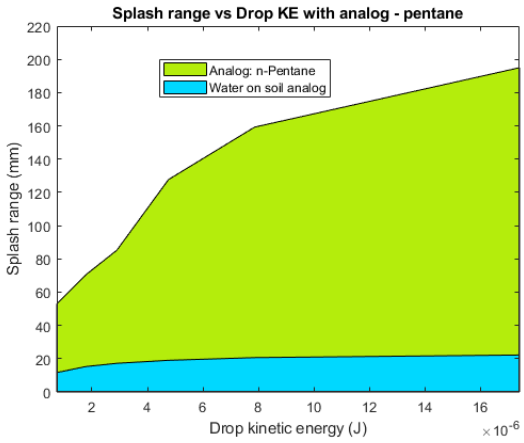

(b) Measurements made using n-pentane as the analog

Figure 9.10: Extent of splash ranges for soil particles on Titan. These values are compared to the diameter of splash circles made by water on Earth, to serve as a suitable comparison between the performance of the two rain liquids

Furthermore, since the quadratic model records much higher splash ratios, the ranges obtained using the quadratic models have not been shown here since it is impossible to visualise the ranges made possible by water in the same plot. However, since it has been established that the linear model is a lower boundary for the behaviour of the splashed particles, it must be understood that the actual flight ranges can be a little higher than the boundary lines shown in Fig. 9.10a and Fig. 9.10b. These figures only seek to highlight how much higher the splash ranges on Titan might be in comparison to what it might be on Earth. Ergo, a slight increase in splash ranges for water, for example in each plot set will correlate a similar increase for respective analog. This means that the scale of comparison

for splash ranges for both analogs in comparison to water is relevant and is what must be highlighted in both figures. However, to get a complete picture of erosive influence, the splash ranges must be compared to how water displaces soil on Earth. This is shown in the validation section below.

9.4. Validation

The comparison to water splashing on soil analogs on Earth hold any integrity only if the measured values are comparable to actual values measured on Earth. The previous section only aimed to highlight the erosive capability of rain on Titan in contrast to water while performing on the soil equivalent of Titan. For the comparison of erosive performance, the splash/drop energy ratios have been used as a metric. For water drops falling at terminal velocity on Earth and splashing on level soil of various types that are available on Earth, Ghadiri *et al.* [25, 24] and Marzen *et al.* [39] have demonstrated that splashing material carries away approximately on average, 10% to 25% of the energy of the drop. This is shown in comparison to the performance of the drop below in Fig. 9.11a, 9.11b, 9.11c.

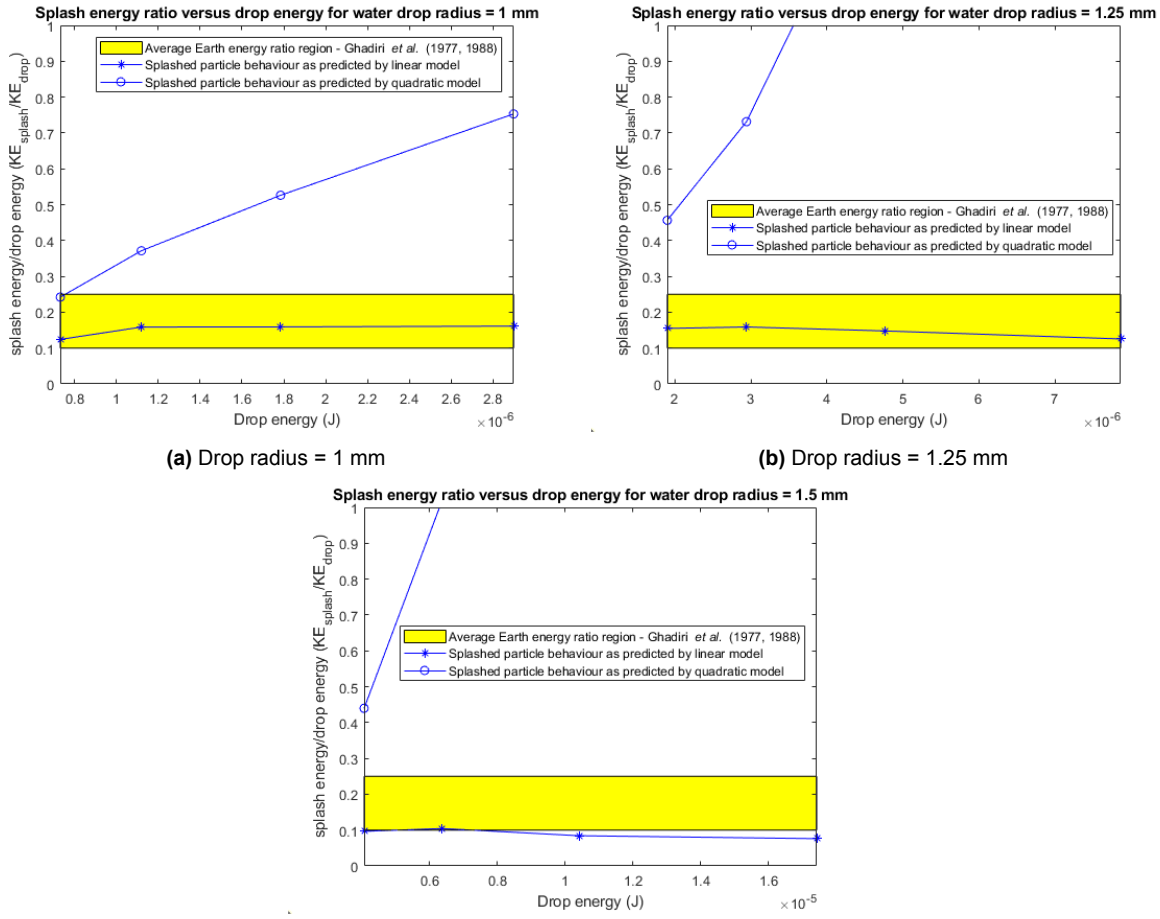

(a) Drop radius = 1 mm

(b) Drop radius = 1.25 mm

(c) Drop radius = 1.5 mm

Figure 9.11: Comparison of splash to drop energy ratio of water on soil analog versus values measured for rain drop on Earth's soil experiments

This indicates that the properties of water are fairly consistent in its interaction with the soil on Earth or with analogs to represent soil on Titan. This is a conclusion drawn from the fact that the lower boundary is almost always within the range described by literature. The possibility of the energy ratios being higher than this Earth based range (made possible by the very high upper boundary defined by the quadratic model) is coherent because the soil is of much lower particle density and consists of much lower cohesive forces binding the particles together compared to traditional soil or even sand. However, it can be seen that the trend lines for quadratic models in all cases exceed 1, which violates the law of conservation of energy. Also, the curves for the linear model fall very much within the boundary

defined by literature for water on Earth, meaning that the linear model works best to explain drop-soil interaction to a better accuracy. This means that even though the high surface tension of water prevents the energy transfer that the analogs initiate, the energy transferred is still possibly on the high end (or higher) than normal soil. The reason for this is beyond the scope of this thesis and can be attempted to answer in the work carried out in the future, on the topic of Titan's soil.

9.5. Discussion

The plots showing the ratio of splash energy to drop energy (Fig. 9.7, 9.8, 9.9) show that the amount of energy being carried away from the drop increases with increasing drop size and with increasing drop size, increasing drop height (seen by increasing drop energy in the X axis of the plots) also contributes to a greater increase in splash energy. The deviation from water is especially notable, considering that at lower drop sizes (drop radius = 1 mm), the splash-drop energy ratio is comparable between water and ethanol, with both of them lying in the 0.15-0.2 range. N-Pentane however, still shows a distinct performance showing an energy ratio consistently in the 0.25 range across all drop energies. Models predict that for a drop of 1.5 mm radius, both analogs differ from of water and contribute to a significant amount of the drop's energy being carried away by the splashing soil at higher drop energies, meaning for larger drops, falling from a greater height implies a greater probability of soil erosion. Drop size appears to be relatively independent for drops falling from a height of 10 km as n-pentane records a ratio of 0.25 while ethanol records 0.1-0.15 (performing consistently on par with water). This means that the erosive capability of rain liquid on Titan is on par with Earth. This conclusion comes from the validation section, where it can very clearly be seen that the energy carried away by the splashing soil is on par with **This also means that if rain is a global phenomenon, splash erosion is a very strong possibility on Titan** since water contributes to substantial splash erosion on Earth.

For larger drops, the impact of splash erosion is further substantial. Combined with increased splash-drop energy ratios as seen in Fig. 9.7, 9.8, 9.9, the plots shown in Fig. A.2, A.3, A.5, A.6 reflect on the increased splashing ranges as well. To put in numerical context, water splashed the soil samples on Earth in the range of 5 - 11 mm (across all drop sizes and fall heights) while the simulation results mention a splash range of 20 - 100 mm as a lower boundary (ranges defined by velocities obtained from the linear model) while indicating the possibility of splash ranges being as high as 500 mm. These numbers only seek to put into context, the erosive capability of rain liquid on Titan versus rain liquid on Earth, pointing to a probable conclusion that **not only is rain on Titan contributing significantly to soil erosion, but also is responsible for significantly displacing soil in a local scale, through immediate impact, on Titan**. It must also remembered that much larger drops also fall on Titan (until drop radius of 3 mm), meaning there is much more to uncover and if the existing plots point towards any trend, it is that larger drops will further displace soil. But that is a conclusion that can definitely be made only with future experimentation. To add to this, we have seen what a single drop is capable of doing, so further experimentation on rain showers will shed light into how much of a contributor rain on Titan is to its sediment transport mechanism.

Therefore, in future missions to Titan, different nature of soil in different locations on Titan will point to the possibility of rain having occurred in certain places and further experimentation from future missions will help classify different kinds of soil better. This further will develop better landing sites for future exploration on Titan.

9.6. Future work

1. Experimenting with larger drops until drop radius = 3 mm
2. Experimenting with various grain sizes of glass bubbles to better capture the response of soil particles to splashing rain drops
3. Experimenting with different cohesive forces among soil particle analogs to better understand how energy transfer can be dependant on the cohesive forces on Titan, and how that is different to the similar relation on Earth, due to the different environmental conditions.
4. Performing experiments to study the influence of rain showers as an extension of the influence of a single rain drop

5. Completely eliminate wind through constriction barriers - the current fumehood and its restrictions meant that it was not possible to create a restriction to air flow without causing vortices that disturbed the upper layers of the soil analog samples.

10

I henceforth conclude...

10.1. Research Question

It now remains, to answer the research question that initiated the chain of events during the course of this thesis. The question that was asked was

What are the qualitative and quantitative differences between rainfall on Earth and Titan and how does this difference reflect on the impact the drops have on soil?

From a qualitative perspective, it is fair to conclude that a single drop of rain on Titan displaces soil to a greater distance than a water drop does on Earth. Combined with the distance, the soil on Titan carries away a greater percentage of the drop's energy than splashing soil on Earth does. This means that there is a better prospect of subsequent energy transfer through secondary impact of splashing soil particles with other soil particles at rest. It is possible to conclude that since there is greater amount of energy being carried away by the soil, there is a greater transfer of soil particles *en masse* during a rain shower. This means that rain on Titan, if existing in regular intervals, would serve as a significant contributor to the soil transport mechanism on Titan.

From a quantitative perspective, it can be seen that not only does a rain drop on Titan contribute to greater displacement of soil particles in comparison to water, had it rained drops of water on Titan. Not only does it contribute to greater displacement but also, to greater percentage of energy being carried away from the drops to soil particles. This could also mean that there is greater energy being subsequently transferred to other soil particles that the splashed particles interact with, meaning in a rain shower, there could be substantial displacement of soil particles because of the significantly higher amount of energy they carry away from the rain drop (in contrast to water on both, the soil analog and water on soil - an average estimate).

10.2. Research Objectives

This section aims to answer the research objectives that were set out to achieve as a part of this thesis work. It is outlined as follows

Estimating possible composition of rain on Titan
From data gathered and evidence laid out in Chapter 4, it has been established that a rain drop falling on the surface of Titan contains approximately, by mole fraction, **77% of methane and 23% of nitrogen**.

Evaluating if it is possible to obtain analogs of rain and soil to replicate Titan's rainfall in a laboratory
On establishing the parameters that need to remain constant (surface tension) and calculating the value of other parameters that would vary due to the changing conditions between Titan and Earth, it has been explained in Chapter 5 that there are two possible chemical compounds that could serve as analogs to replicate the behaviour of a rain drop falling on Titan, on Earth. These two are

1. Ethanol (C_2H_6O)
2. n-Pentane (C_5H_{12})

Furthermore, it was concluded that the usage of glass bubbles that consist of an average diameter of 65 μm would suffice in order to mimic the behaviour of Titan's soil in Earthly experimental setups.

Measuring parameters that define splash erosion on Titan
A conclusion for this deliberation has been provided in Chapter 6. Based on data that would be relevant to continue to evaluate the energy carried away by the splashing soil, it was determined that two parameters were necessary to be measured in order to define splash erosion on Titan, in the lab based experiments. They are

1. Crater diameter produced by impacting drop
2. Splash circle diameter produced by splashing soil generated by impacting drop

Building models that predict the behaviour of soil on Titan after being subject to splash erosion
In order to predict the behaviour of a splashing particle and how much energy the splashing particles were carrying away together, two mathematical models were built. They are listed below

1. Soil particle trajectory simulation model
2. Drop energy split simulation model

Both these models were instrumental in determining how much velocity and energy the soil was carrying away from the energy brought to the soil by the impacting drop. The models are broken down and reasoned about in Chapter 7.

From a quantitative perspective, it is possible to conclude that the distances soil will move is much higher than what it would be on Earth. However, this is an answer better provided by the results of experiments made to observe the behaviour of soil after being subject to continuous rain showers in different intervals. In order to better quantify the influence of rain on soil erosion, further work needs to be done. This is listed below

1. Experimenting with increased drop sizes (drop radius range 2 - 3 mm)
2. Experimenting with rain showers at different frequency to observe washout rate of soil from multiple drops
3. Experimenting with soil analogs of different grain sizes ($\sim$ 30 - 250 μm)

Thus, it remains to be seen, the impact rain can have on the soil while splashing. However, the initial results obtained from the single drop experiments alone are exciting when put in context of splash ranges and energies because of the prospect of a soil transport mechanism of splash erosion that is possibly much stronger than what we have on Earth. It is possible to imagine swathes of soil being transported away during a rain shower on Titan and if the frequency of rain on Titan is established to a greater certainty, then it is possible to estimate how much soil can be transported and further, use that as a signature to identify from soil appearance, the behaviour and existence of rain at a certain location on Titan. However, for now, the results of this thesis, when put in perspective, will appear in a manner as detailed in the following section.

10.3. Perspective

The rain on Titan, while slow and consisting of large drops, also experiences considerable evaporation in the scenario of heavy showers before they hit the ground [26]. This means that rain-watching could be an activity on Titan, where you could lie down on the ground for a short period of time and watch rain falling in slow-motion (from an Earth based perspective) only for it to vaporise before it reaches you. However, the drops that reach the surface will ensure that you cannot stay for long, since they would cover you in soil very quickly. Camping in a tent would not help much either. For perspective, typically, a medium shower on Earth would result in the walls of tents looking something like this (Fig 10.1) after a good 3-4 hours of showering.

Figure 10.1: A tent after a medium shower on Earth. Source: Getty images

After a 3-4 hour shower of mild to medium rain on Titan, your tent could very well end up looking like the one in Fig. 10.2

Figure 10.2: A purported estimation of how it might look after an equally medium shower on Titan. Source: www.grist.org

Figure 10.3: What you would probably look like if you went out biking in a ”mild drizzle” on Titan. Source: www.britishcycling.org.uk/mtb/article/mtb20120503-mountain-bike-Mud-Sweat-and-Gears-Eastern-MTB-Series-Round-2-0

The fact that rain can considerably impact the soil movement on Titan is a very interesting feature and simply the presence of rain as a global phenomenon will imply the presence of many Earth like features to exist on Titan, such as soil transport, soil organic composition and sediment circulation from within the sub soil due to displacing soil occurring from rain drop splashing.

References

[1] 3M. *Energy and Advanced Materials Division Bubbles 3M ™ Glass Mikro-Glashohlkugeln Produktinformation und Spezifikation Europäische Produktion nach ISO 9001 : 2000*. Tech. rep.

[2] *Air Pollution - Maximum Mixing Depth and Ventilation Coefficient | Atmosphere Of Earth | Altitude*. URL: https://www.scribd.com/doc/35920824/Air-Pollution-Maximum-Mixing-Depth-and-Ventilation-Coefficient.

[3] V. G. Baidakov and M. N. Khotienkova. "Surface tension of methane–nitrogen solutions: 2. Description in the framework of the van der Waals gradient theory". In: *Fluid Phase Equilibria* 425 (Oct. 2016), pp. 402–410. ISSN: 03783812. DOI: 10.1016/j.fluid.2016.06.038.

[4] Erika L. Barth and Owen B. Toon. "Methane, ethane, and mixed clouds in Titan's atmosphere: Properties derived from microphysical modeling". In: *Icarus* 182.1 (May 2006), pp. 230–250. ISSN: 00191035. DOI: 10.1016/j.icarus.2005.12.017.

[5] Erika L. Barth and Owen B. Toon. *Microphysical modeling of ethane ice clouds in Titan's atmosphere*. Mar. 2003. DOI: 10.1016/S0019-1035(02)00067-2.

[6] Erika L. Barth and Owen B. Toon. "Properties of methane clouds on Titan: Results from microphysical modeling". In: *Geophysical Research Letters* 31.17 (Sept. 2004), n/a–n/a. ISSN: 00948276. DOI: 10.1029/2004GL019825. URL: http://doi.wiley.com/10.1029/2004GL019825.

[7] Reginald Christian Bernardo et al. "Wind-influenced projectile motion". In: *European Journal of Physics* 36.2 (Feb. 2015), p. 025016. ISSN: 0143-0807. DOI: 10.1088/0143-0807/36/2/025016. URL: https://iopscience.iop.org/article/10.1088/0143-0807/36/2/025016%20https://iopscience.iop.org/article/10.1088/0143-0807/36/2/025016/meta.

[8] W. J. Borucki and R. C. Whitten. "Influence of high abundances of aerosols on the electrical conductivity of the Titan atmosphere". In: *Planetary and Space Science* 56.1 (Jan. 2008), pp. 19–26. ISSN: 0032-0633. DOI: 10.1016/J.PSS.2007.03.013.

[9] Devon M. Burr et al. "Higher-than-predicted saltation threshold wind speeds on Titan". In: *Nature* 517.7532 (Jan. 2015), pp. 60–63. ISSN: 14764687. DOI: 10.1038/NATURE14088.

[10] Devon M. Burr et al. "The Titan Wind Tunnel: A new tool for investigating extraterrestrial aeolian environments". In: *Aeolian Research* 18 (Sept. 2015), pp. 205–214. ISSN: 1875-9637. DOI: 10.1016/J.AEOLIA.2015.07.008.

[11] Peter Chudinov. "An Optimal Angle of Launching a Point Mass in a Medium with Quadratic Drag Force". In: (June 2005). DOI: 10.48550/arxiv.physics/0506201. URL: https://arxiv.org/abs/physics/0506201v1.

[12] Peter Chudinov. "Approximate Analytical Description of the Projectile Motion with a Quadratic Drag Force". In: *ATHENS JOURNAL OF SCIENCES* 1.2 (May 2014), pp. 97–106. DOI: 10.30958/AJS.1-2-2.

[13] Peter S. Chudinov. "The Motion of a Heavy Particle in a Medium with Quadratic Drag Force". In: *International Journal of Nonlinear Sciences and Numerical Simulation* 3.2 (2002), pp. 121–129. ISSN: 15651339. DOI: 10.1515/IJNSNS.2002.3.2.121.

[14] C. D. Collinson and T. Roper. "Stokes Drag". In: *Particle mechanics* (1995), p. 30.

[15] Athena Coustenis. "The origin and evolution of Titan's atmosphere". In: ().

[16] Athena Coustenis. "Titan". In: *Encyclopedia of the Solar System*. Elsevier Inc., Jan. 2007, pp. 467–482. ISBN: 9780120885893. DOI: 10.1016/B978-012088589-3/50029-3.

[17] Athena Coustenis. "What Cassini-Huygens has revealed about Titan". In: *Astronomy and Geophysics* 48.2 (Apr. 2007), pp. 14–2. ISSN: 14684004. DOI: 10.1111/j.1468-4004.2007.48214.x. URL: https://academic.oup.com/astrogeo/article-lookup/doi/10.1111/j.1468-4004.2007.48214.x.

[18] Athena Coustenis et al. *Titan's atmosphere from ISO mid-infrared spectroscopy*. Feb. 2003. DOI: 10.1016/S0019-1035(02)00028-3.

[19] A. I. J. M. van Dijk, A. G. C. A. Meesters, and L. A. Bruijnzeel. "Exponential Distribution Theory and the Interpretation of Splash Detachment and Transport Experiments". In: *Soil Science Society of America Journal* 66.5 (Sept. 2002), pp. 1466–1474. ISSN: 03615995. DOI: 10.2136/SSSAJ2002.1466.

[20] Herman Erlichson. "Maximum projectile range with drag and lift, with particular application to golf". In: *American Journal of Physics* 51.4 (Apr. 1983), pp. 357–362. ISSN: 0002-9505. DOI: 10.1119/1.13248.

[21] Daniel G Friend, James F Ely, and Hepburn Ingham. "An Empirical Equation for Thermodynamic Properties of Light Hydrocarbons and Their Mixtures I. Methane, Ethane". In: *Thermophysical Properties of Fluids. II. Methane, Ethane, Propane, Isobutane, and Normal Butane Journal of Physical and Chemical Reference Data* 18 (1989), p. 334. DOI: 10.1063/1.555828. URL: https://doi.org/10.1063/1.55582818,583https://doi.org/10.1063/1.1750658.

[22] M. Fulchignoni et al. "In situ measurements of the physical characteristics of Titan's environment". In: *Nature 2005 438:7069* 438.7069 (Nov. 2005), pp. 785–791. ISSN: 1476-4687. DOI: 10.1038/nature04314. URL: https://www.nature.com/articles/nature04314.

[23] *Fundamentals of Atmospheric Modeling - Mark Z. Jacobson, Professor Mark Z Jacobson - Google Books*. URL: https://books.google.nl/books?hl=en&lr=&id=QnzHkFN3v8AC&oi=fnd&pg=PR11&ots=iga4iJsMUc&sig=ZpG1fCSsBHDwgEA9bUTuCMhKPQU&redir_esc=y#v=onepage&q&f=false.

[24] H. GHADIR and D. PAYNE. "The formation and characteristics of splash following raindrop impact on soil". In: *Journal of Soil Science* 39.4 (1988), pp. 563–575. ISSN: 13652389. DOI: 10.1111/J.1365-2389.1988.TB01240.X.

[25] H. GHADIRI and D. PAYNE. "RAINDROP IMPACT STRESS AND THE BREAKDOWN OF SOIL CRUMBS". In: *Journal of Soil Science* 28.2 (1977), pp. 247–258. ISSN: 13652389. DOI: 10.1111/J.1365-2389.1977.TB02233.X.

[26] S. D.B. Graves et al. "Rain and hail can reach the surface of Titan". In: *Planetary and Space Science* 56.3-4 (Mar. 2008), pp. 346–357. ISSN: 00320633. DOI: 10.1016/j.pss.2007.11.001.

[27] *Hazardous Substances Data Bank (HSDB) - PubChem Data Source*. URL: https://pubchem.ncbi.nlm.nih.gov/source/Hazardous%20Substances%20Data%20Bank%20(HSDB).

[28] Chao He et al. "Carbon Monoxide Affecting Planetary Atmospheric Chemistry". In: *The Astrophysical Journal Letters* 841.2 (June 2017), p. L31. ISSN: 2041-8205. DOI: 10.3847/2041-8213/AA74CC. URL: https://iopscience.iop.org/article/10.3847/2041-8213/aa74cc%20https://iopscience.iop.org/article/10.3847/2041-8213/aa74cc/meta.

[29] S. M. Hörst. *Titan's atmosphere and climate*. Mar. 2017. DOI: 10.1002/2016JE005240. URL: https://agupubs.onlinelibrary.wiley.com/doi/full/10.1002/2016JE005240%20https://agupubs.onlinelibrary.wiley.com/doi/abs/10.1002/2016JE005240%20https://agupubs.onlinelibrary.wiley.com/doi/10.1002/2016JE005240.

[30] S. M. Hörst and M. A. Tolbert. "IN SITU MEASUREMENTS OF THE SIZE AND DENSITY OF TITAN AEROSOL ANALOGS". In: *The Astrophysical Journal Letters* 770.1 (May 2013), p. L10. ISSN: 2041-8205. DOI: 10.1088/2041-8205/770/1/L10. URL: https://iopscience.iop.org/article/10.1088/2041-8205/770/1/L10%20https://iopscience.iop.org/article/10.1088/2041-8205/770/1/L10/meta.

[31] Hiroshi Imanakaa and Mark A. Smith. "Formation of nitrogenated organic aerosols in the Titan upper atmosphere". In: *Proceedings of the National Academy of Sciences of the United States of America* 107.28 (July 2010), pp. 12423–12428. ISSN: 00278424. DOI: 10.1073/pnas.0913353107. URL: www.pnas.org/cgi/doi/10.1073/pnas.0913353107.

[32] *In Depth | Titan – NASA Solar System Exploration*. URL: https://solarsystem.nasa.gov/moons/saturn-moons/titan/in-depth/.

[33] Jean Pierre Lebreton et al. “An overview of the descent and landing of the Huygens probe on Titan”. In: *Nature 2005 438:7069* 438.7069 (Nov. 2005), pp. 758–764. ISSN: 1476-4687. DOI: 10.1038/nature04347. URL: https://www.nature.com/articles/nature04347.

[34] Sophie Leguédois et al. “Splash Projection Distance for Aggregated Soils”. In: *Soil Science Society of America Journal* 69.1 (2005), p. 30. DOI: 10.2136/SSSAJ2005.0030.

[35] Kimberly L. Litwin et al. “Influence of temperature, composition, and grain size on the tensile failure of water ice: Implications for erosion on Titan”. In: *Journal of Geophysical Research: Planets* 117.E8 (Aug. 2012), p. 8013. ISSN: 2156-2202. DOI: 10.1029/2012JE004101. URL: https://onlinelibrary.wiley.com/doi/full/10.1029/2012JE004101%20https://onlinelibrary.wiley.com/doi/abs/10.1029/2012JE004101%20https://agupubs.onlinelibrary.wiley.com/doi/10.1029/2012JE004101.

[36] Lyle N. Long and Howard Weiss. “The Velocity Dependence of Aerodynamic Drag: A Primer for Mathematicians”. In: *The American Mathematical Monthly* 106.2 (Feb. 1999), pp. 127–135. ISSN: 0002-9890. DOI: 10.1080/00029890.1999.12005019.

[37] Ralph D Lorenz. *The life, death and afterlife of a raindrop on Titan*. Tech. rep. 9. 1993, pp. 647–655.

[38] Ralph D. Lorenz. “Titan: Interior, surface, atmosphere, and space environment, edited by I. Müller-Wodarg, C. A. Griffith, E. Lellouch, and T. E. Cravens. Cambridge, UK: Cambridge University Press, 2014, 474 p. $135, hardcover (ISBN #978-0521199926).” In: *Meteoritics & Planetary Science* 49.6 (June 2014), pp. 1139–1140. ISSN: 1945-5100. DOI: 10.1111/MAPS.12317. URL: https://onlinelibrary.wiley.com/doi/full/10.1111/maps.12317%20https://onlinelibrary.wiley.com/doi/abs/10.1111/maps.12317%20https://onlinelibrary.wiley.com/doi/10.1111/maps.12317.

[39] Miriam Marzen and Thomas Iserloh. “Processes of raindrop splash and effects on soil erosion”. In: *Precipitation: Earth Surface Responses and Processes* (Jan. 2021), pp. 351–371. DOI: 10.1016/B978-0-12-822699-5.00013-6.

[40] L. Mouzai and M. Bouhadef. “Shear strength of compacted soil: Effects on splash erosion by single water drops”. In: *Earth Surface Processes and Landforms* 36.1 (Jan. 2011), pp. 87–96. ISSN: 01979337. DOI: 10.1002/ESP.2021.

[41] *NASA delays Dragonfly launch by a year - SpaceNews*. URL: https://spacenews.com/nasa-delays-dragonfly-launch-by-a-year/.

[42] H. B. Niemann et al. “Composition of Titan’s lower atmosphere and simple surface volatiles as measured by the Cassini-Huygens probe gas chromatograph mass spectrometer experiment”. In: *Journal of Geophysical Research* 115.E12 (Dec. 2010), E12006. ISSN: 0148-0227. DOI: 10.1029/2010JE003659. URL: http://doi.wiley.com/10.1029/2010JE003659.

[43] H. B. Niemann et al. “The abundances of constituents of Titan’s atmosphere from the GCMS instrument on the Huygens probe”. In: *Nature* 438.7069 (Dec. 2005), pp. 779–784. ISSN: 14764687. DOI: 10.1038/nature04122. URL: https://www.nature.com/articles/nature04122.

[44] J. Poesen and J. Savat. “Detachment and transportation of loose sediments by raindrop splash: Part II Detachability and transport ability measurements”. In: *CATENA* 8.1 (Jan. 1981), pp. 19–41. ISSN: 0341-8162. DOI: 10.1016/S0341-8162(81)80002-1.

[45] Carolyn C. Porco et al. “Imaging of Titan from the Cassini spacecraft”. In: *Nature* 434.7030 (Mar. 2005), pp. 159–168. ISSN: 00280836. DOI: 10.1038/nature03436. URL: www.nature.com/nature.

[46] W. Reid Thompson, John A. Zollweg, and David H. Gabis. “Vapor-liquid equilibrium thermodynamics of N2 + CH4: Model and Titan applications”. In: *Icarus* 97.2 (June 1992), pp. 187–199. ISSN: 10902643. DOI: 10.1016/0019-1035(92)90127-S.

[47] H. Th Riezebos and G.F Epema. “Drop shape and erosivity. Part II: Splash detachment, splash transport and erosivity indices.” In: *Earth Surface Processes and Landforms* 10 (1985), pp. 69–74.

[48] *Sediment transport - Wikipedia*. URL: https://en.wikipedia.org/wiki/Sediment_transport.

[49] G. G. Stokes. “On the effect of internal friction of fluids on the motion of pendulums”. In: *Transactions of the Cambridge Philosophical Society* 9, part ii (1851), pp. 8–106. URL: https://babel.hathitrust.org/cgi/pt?id=mdp.39015012112531;view=1up;seq=208.

[50] Thomas R Strobridge. *THE THERMODYNAMIC PROPERTIES OF NITROGEN FROM 64 TO 300 K BETWEEN 0.1 AND 200 ATMOSPHERES*. Tech. rep. NATIONAL BUREAU OF STANDARDS, 1962. DOI: 10.6028/NBS.TN.129. URL: https://nvlpubs.nist.gov/nistpubs/Legacy/TN/nbstechnicalnote129.pdf.

[51] Peter Timmerman and Jacobus P. van der Weele. “On the rise and fall of a ball with linear or quadratic drag”. In: *American Journal of Physics* 67.6 (May 1999), p. 538. ISSN: 0002-9505. DOI: 10.1119/1.19320. URL: https://aapt.scitation.org/doi/abs/10.1119/1.19320.

[52] T. Tokano, F. M. Neubauer, and R. D. Lorenz. “Tidal winds on Titan: measurement goals and mobility opportunities for future missions”. In: *Proceedings of the First European Workshop on Exo-Astrobiology* (Sept. 2002), pp. 353–355.

[53] Tetsuya Tokano. “Latitudinal Distribution of Ethane Precipitation on Titan Modulated by Topography and Orbital Forcing and Its Implication for Titan’s Surface Evolution”. In: *The Planetary Science Journal* 2 (2021), p. 86. DOI: 10.3847/PSJ/abf049. URL: https://doi.org/10.3847/PSJ/abf049.

[54] Tetsuya Tokano and Fritz M. Neubauer. “Tidal winds on Titan caused by Saturn”. In: *Icarus* 158.2 (Aug. 2002), pp. 499–515. ISSN: 00191035. DOI: 10.1006/icar.2002.6883.

[55] Tetsuya Tokano et al. “Methane drizzle on Titan”. In: *Nature* 442.7101 (July 2006), pp. 432–435. ISSN: 14764687. DOI: 10.1038/nature04948. URL: https://www.nature.com/articles/nature04948.

[56] M. G. Tomasko et al. “Rain, winds and haze during the Huygens probe’s descent to Titan’s surface”. In: *Nature 2005 438:7069* 438.7069 (Nov. 2005), pp. 765–778. ISSN: 1476-4687. DOI: 10.1038/nature04126. URL: https://www.nature.com/articles/nature04126.

[57] Owen B. Toon et al. “Methane rain on Titan”. In: *Icarus* 75.2 (Aug. 1988), pp. 255–284. ISSN: 10902643. DOI: 10.1016/0019-1035(88)90005-X.

[58] Harish Chandra Verma. “Concepts of physics”. In: (1999).

[59] Eric H. Wilson and Sushil K. Atreya. “Titan’s carbon budget and the case of the missing ethane”. In: *Journal of Physical Chemistry A* 113.42 (Oct. 2009), pp. 11221–11226. ISSN: 10895639. DOI: 10.1021/jp905535a. URL: https://pubs.acs.org/doi/abs/10.1021/jp905535a.

[60] R V Yelle et al. *Engineering Models for Titan’s Atmosphere*. Tech. rep.

[61] Xinting Yu et al. “The effect of adsorbed liquid and material density on saltation threshold: Insight from laboratory and wind tunnel experiments”. In: *Icarus* 297 (Nov. 2017), pp. 97–109. ISSN: 0019-1035. DOI: 10.1016/J.ICARUS.2017.06.034.

[62] John C. Zarnecki et al. “A soft solid surface on Titan as revealed by the Huygens Surface Science Package”. In: *Nature 2005 438:7069* 438.7069 (Nov. 2005), pp. 792–795. ISSN: 1476-4687. DOI: 10.1038/nature04211. URL: https://www.nature.com/articles/nature04211.

A

Trajectory plots

A.0.1. Plots for ethanol analog

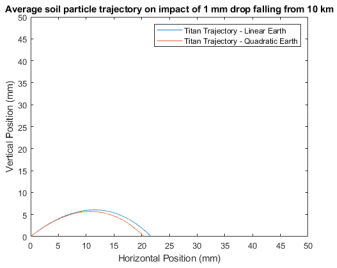

(a) 1 mm, 10 km

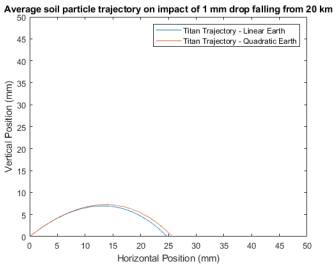

(b) 1 mm, 20 km

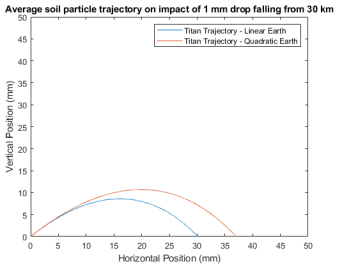

(c) 1 mm, 30 km

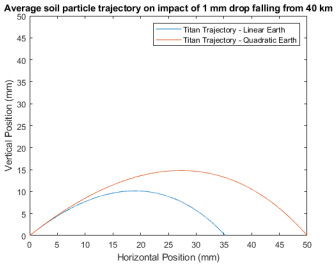

(d) 1 mm, 40 km

Figure A.1: Plots showing the projectile trajectories of a hypothetical soil particle being scattered after a drop (sub caption mentions radius of drop, fall height of drop) has fallen onto it. Initial velocities are obtained taking into account splash diameters generated by **ethanol**

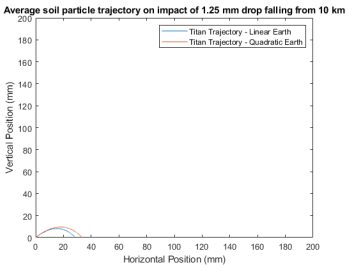

(a) 1.25 mm, 10 km

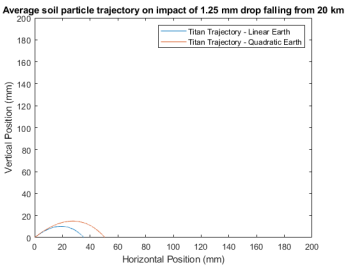

(b) 1.25 mm, 20 km

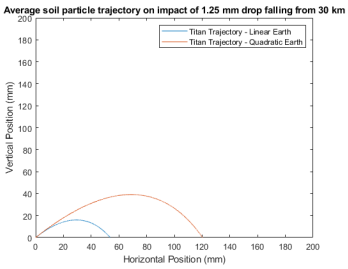

(c) 1.25 mm, 30 km

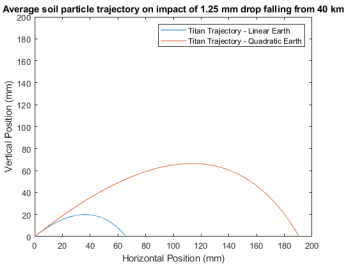

(d) 1.25 mm, 40 km

Figure A.2: Plots showing the projectile trajectories of a hypothetical soil particle being scattered after a drop (sub caption mentions radius of drop, fall height of drop) has fallen onto it. Initial velocities are obtained taking into account splash diameters generated by **ethanol**

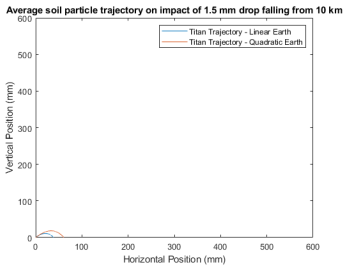

(a) 1.5 mm, 10 km

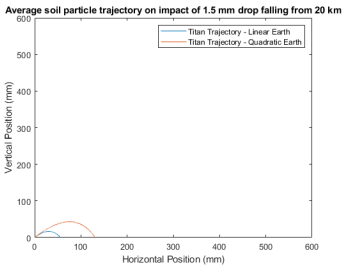

(b) 1.5 mm, 20 km

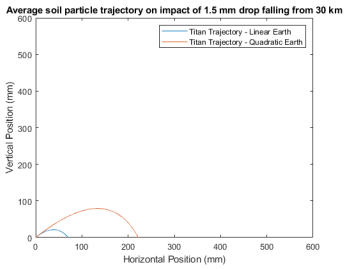

(c) 1.5 mm, 30 km

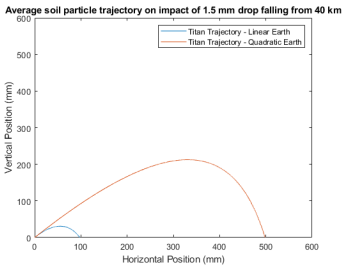

(d) 1.5 mm, 40 km

Figure A.3: Plots showing the projectile trajectories of a hypothetical soil particle being scattered after a drop (sub caption mentions radius of drop, fall height of drop) has fallen onto it. Initial velocities are obtained taking into account splash diameters generated by **ethanol**

A.0.2. Plots for n-pentane analog

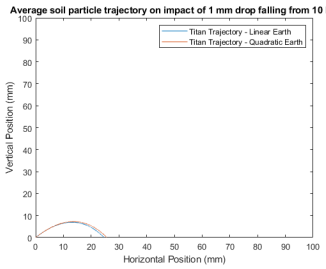

(a) 1 mm, 10 km

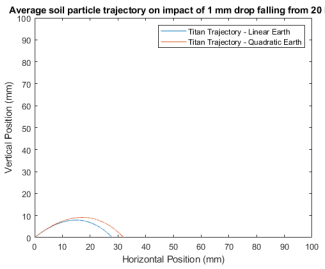

(b) 1 mm, 20 km

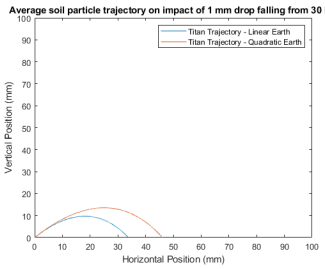

(c) 1 mm, 30 km

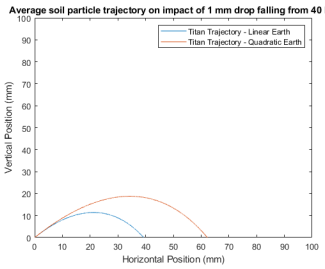

(d) 1 mm, 40 km

Figure A.4: Plots showing the projectile trajectories of a hypothetical soil particle being scattered after a drop (sub caption mentions radius of drop, fall height of drop) has fallen onto it. Initial velocities are obtained taking into account splash diameters generated by **n-pentane**

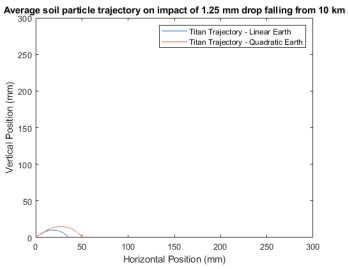

(a) 1.25 mm, 10 km

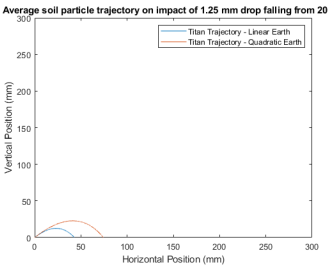

(b) 1.25 mm, 20 km

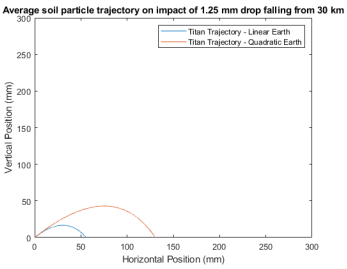

(c) 1.25 mm, 30 km

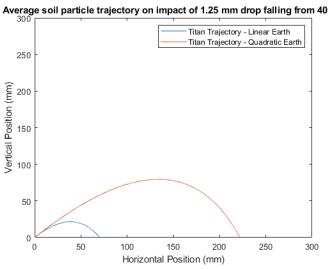

(d) 1.25 mm, 40 km

Figure A.5: Plots showing the projectile trajectories of a hypothetical soil particle being scattered after a drop (sub caption mentions radius of drop, fall height of drop) has fallen onto it. Initial velocities are obtained taking into account splash diameters generated by **n-pentane**

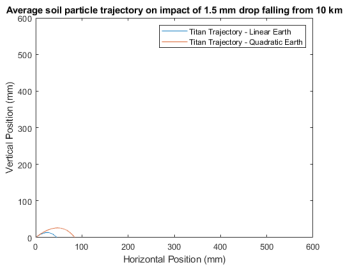

(a) 1.5 mm, 10 km

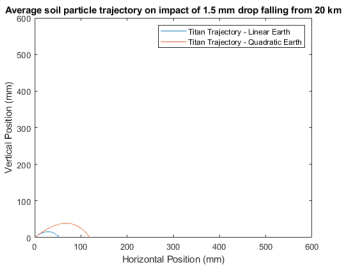

(b) 1.5 mm, 20 km

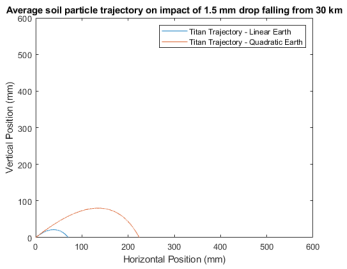

(c) 1.5 mm, 30 km

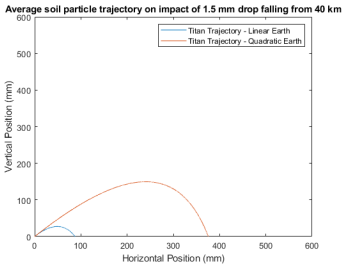

(d) 1.5 mm, 40 km

Figure A.6: Plots showing the projectile trajectories of a hypothetical soil particle being scattered after a drop (sub caption mentions radius of drop, fall height of drop) has fallen onto it. Initial velocities are obtained taking into account splash diameters generated by **n-pentane**

B

Crater diameter versus drop velocity plots

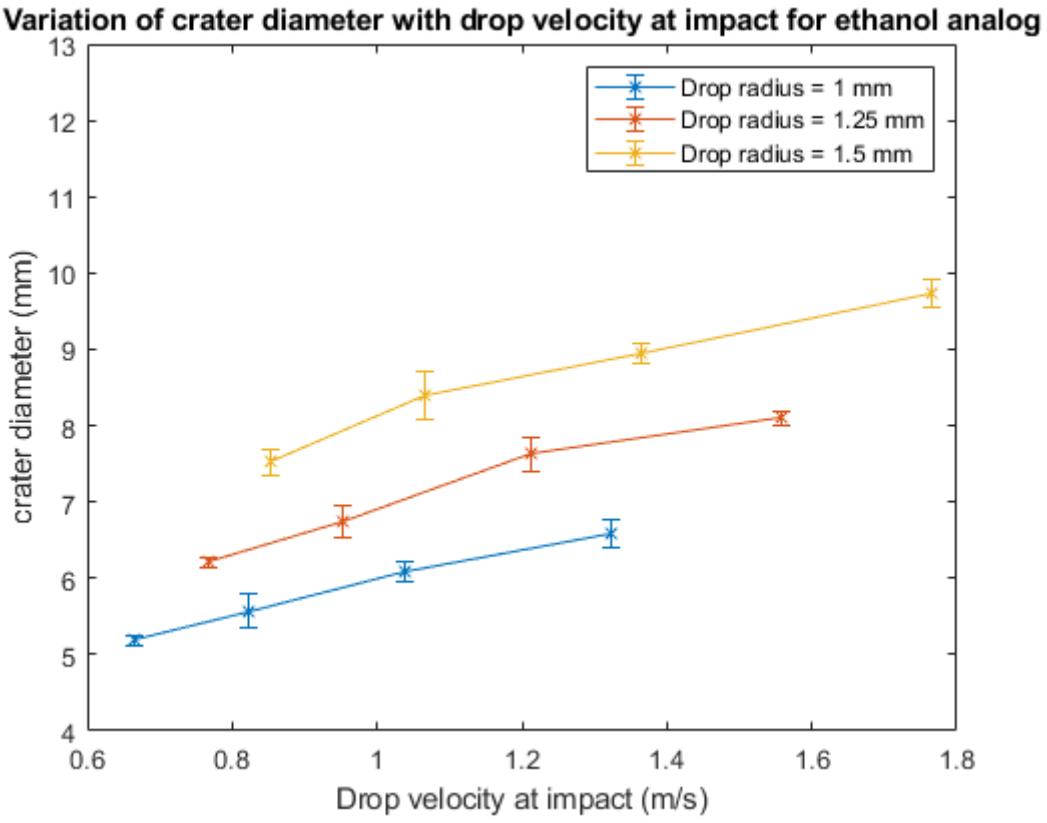

Figure B.1: Crater diameter versus drop velocity for ethanol analog

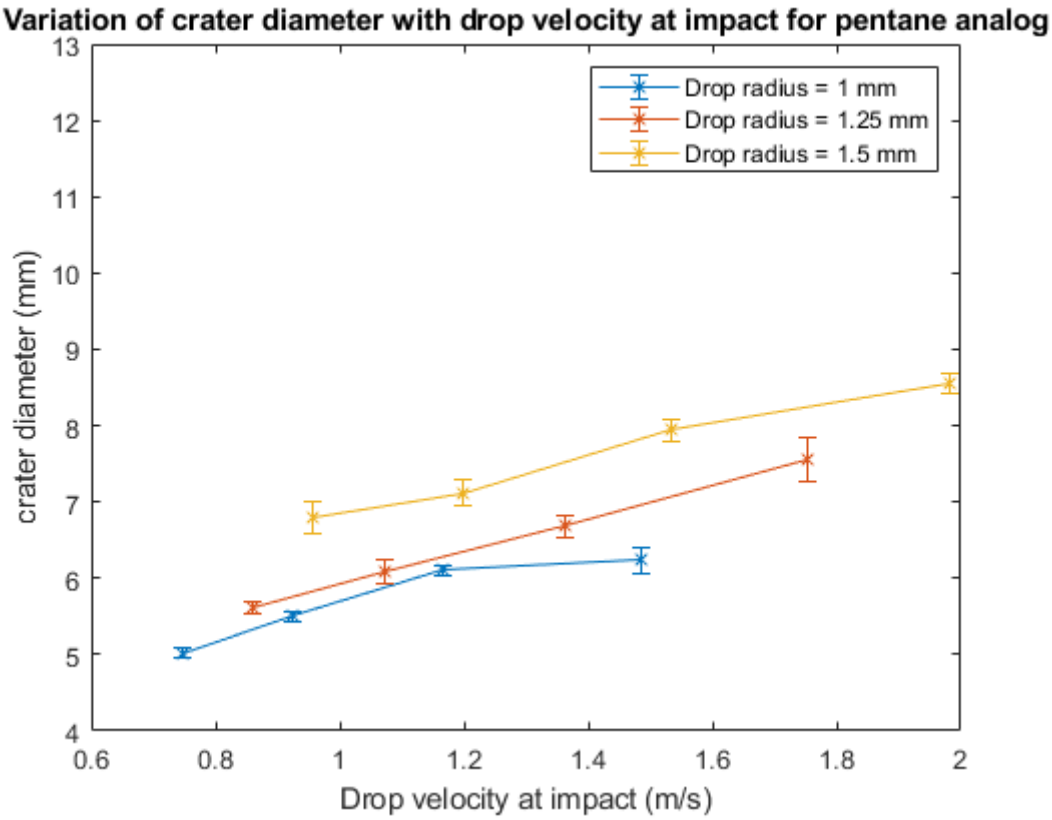

Figure B.2: Crater diameter versus drop velocity for n-pentane analog

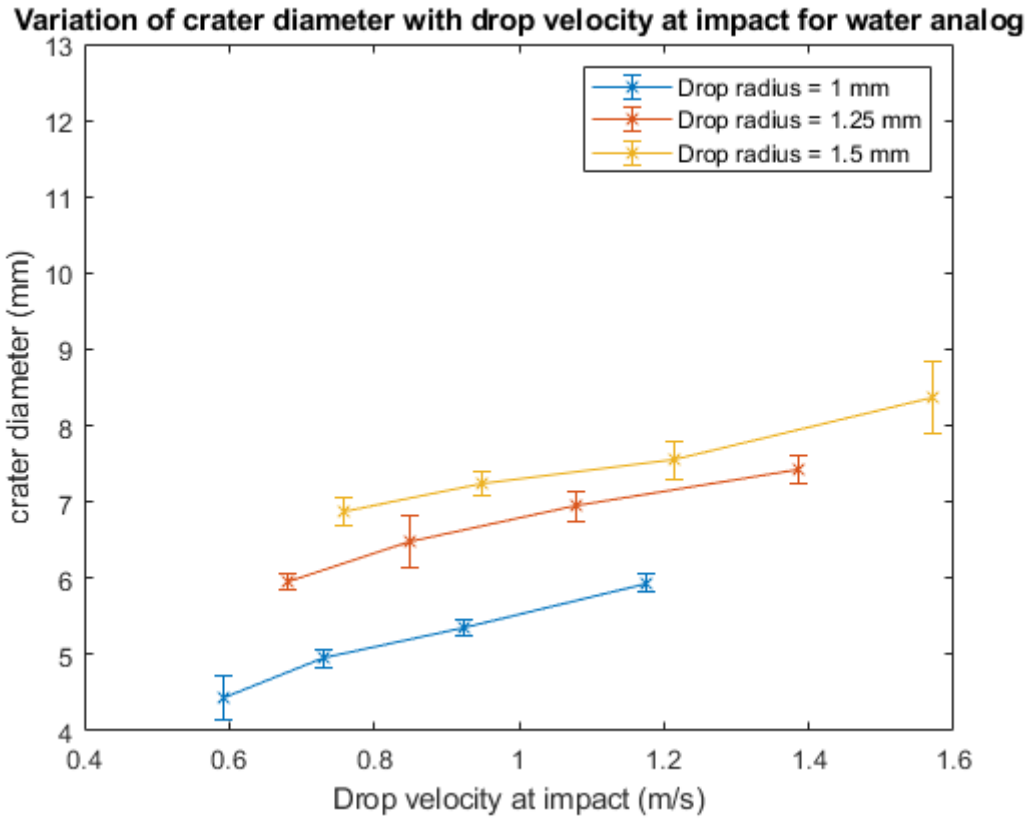

Figure B.3: Crater diameter versus drop velocity for water analog